Improved leaf biochemical constituent retrieval using the theory of spectral invariants to correct hyperspectral remote sensing data for canopy structural effects

Master's Thesis (GEO 511)

Claudio Henry

10-725-455

Submitted: 30.9.2015

Supervisor: Dr. rer. nat. Alexander Damm

Responsible faculty member: Prof. Dr. sc. nat. Michael E. Schaepman

Abstract

Ecosystems deliver essential goods and services for human welfare. The measurement and monitoring of ecosystem properties, therefore, represent vital necessities, especially in times of global changes as today. Remote sensing has the ability to deliver relatively direct measurements of key ecosystem properties with a stable and strong predictive response to ecosystem functions. However, challenges are encountered when using measured reflectance data of vegetation canopy since the signal from the leaf albedo is modulated by the canopy structure. No direct conclusion on ecosystem properties like plant traits can thus be drawn without a model accounting for canopy structure. In this thesis, the retrieval of structural and leaf biochemical parameters is tested using the theory of spectral invariants. The first part analyses sensitivities of retrieved structural parameters across different canopy complexities to test their coherence, underlying assumptions and usability. The second part tries to implement the retrieved structural parameters in a model for the retrieval of leaf biochemical constituents, which accounts for canopy structural effects.

Table of Content

List of Figures

List of tables

1. Introduction

1.1 Context

The goods and services provided by ecosystems represent very important benefits for human (Costanza et al., 1997). Ecosystem services are produced by the activities of organisms, which are linked to organisms by their functional traits (Andrew et al., 2014). Homolová et al. (2013) point out the importance of remote sensing in delivering relatively direct measurements of key ecosystem properties with a stable and strong predictive response to ecosystem functions. An important group of parameters relevant for ecosystem services are the plant traits, which include pigments, dry matter, water, biochemistry content, LAI or LAD (Andrew et al., 2014). Furthermore, the physiological status, plant productivity and nutrients availability of plants is strongly related to their pigment content (Curran, 1989; Gitelson et al., 2006). Monitoring the temporal and spatial dynamics of plant traits is therefore of large interest for environmental and agricultural management (Blackburn, 2007). Spectral reflectance measurements provide a fast and non-destructive technique with considerable progresses made recently by physical and conceptual models in estimating leaf biochemical contents (Sims & Gamon, 2002; Zhang, 2008).

Measured reflectance data, however, is not only influenced by the leaf albedo but is also affected by the canopy structure (Houborg et al., 2015; Rautiainen et al., 2004). Leaf biochemical constituents can therefore not directly be estimated from the measured signal since latter needs correction for canopy structural effects first. There are different canopy reflectance models (Myneni et al., 1995), one being the theory of spectral invariants (Huang et al., 2007; Knyazikhin et al., 1998; Panferov et al., 2001). It is based on the three-dimensional radiative transfer equation of solar radiation interacting with the vegetation canopy and is therefore physically consistent (Knyazikhin et al., 2013). The fact that the interaction probability of photons within the canopy is determined by the canopy structure only results in a wavelength independent behaviour of the vegetation canopy (Knyazikhin et al., 2011). The theory of spectral invariants shows that simple algebraic combinations of the single-scattering albedo and canopy spectral transmittance and reflectance lose their wavelength dependency and determine three canopy structure specific variables – the canopy interceptance, the recollision and escape probabilities (Huang et al., 2007; Panferov et al., 2001). These three spectrally invariant variables can be combined into the directional area scattering factor (DASF), a factor which corrects reflectance data for canopy structural effects (Knyazikhin et al., 2013).

1.2 Motivation

Although the theory of spectral invariants is meanwhile well developed and tested on simulated or remotely sensed spectral data, not many studies have tested the potential of its application. Derivations from the theory of spectral invariants show the possibility to retrieve structural parameters, i. a. the DASF, from hyperspectral data without canopy-reflectance models, prior knowledge, or ancillary information regarding leaf optical properties (Knyazikhin, 2013). The advantage besides not needing any knowledge about the measured canopy is the simplicity of the algorithm underlying the retrieval (Knyazikhin et al., 2013). On the other side, the simplicity also implies assumptions and parts of the theory have been derived from perfectly homogeneous canopies. This could lead to potential issues for the retrieval of structural parameters from real and more complex canopies. The retrieval seems to work so far; however, it was not yet fully tested on observational data of various canopy complexities. Furthermore, no attempt has been made to develop a method for the retrieval of plant traits from spectral measurements, which includes the theory of spectral invariants for the correction of structural effects. Such a retrieval would represent a considerable advance in remote sensing, since no simple solution separating the structural and biochemical portions of a remotely sensed signal without the need of additional information is known today.

1.3 Aims and Objectives

The aim of this thesis is to test the application of the spectral invariants theory for the retrieval of plant traits from remotely sensed high resolution hyperspectral data of different canopy complexities. Therefore, the retrieval of structural variables, namely the DASF, overall recollision probability, p_1, and directional escape probability, R, is first investigated step by step from ideal conditions to complex vegetation canopies. For each degree of canopy complexity the results are compared with the theory and present studies for validity, assumptions are questioned, challenges are shown and the usability of the retrieved structural variables is assigned. With only a few studies to apply the spectral invariants theory on reflectance data, this thesis is to date one of the first to examine the retrieval of the DASF, overall recollision probability and directional escape probability from remotely sensed spectral data. After the evaluation of the retrieval of structural variables, a

method for the retrieval of leaf biochemical constituents derived from the spectral invariants theory and using the retrieved structural variables is tested.

The thesis is subdivided into four parts. In the first one simulated spectra from the PROSAIL model are used to investigate sensibilities of the retrieved structural parameters to different variations of leaf biochemical and canopy structural parameters. The purpose of this part is to have a controlled experiment, although artificial, where each variation of the result can be related to a separate input parameter. It also represents a perfectly homogeneous canopy, which is often an assumption in the derivation of the theory. It is first looked at how the DASF values react to variations of the model parameters. In a second step the sensitivity of the overall recollision probability, p_1, and the directional escape probability, R, to parameter variation is further examined. Lastly, the chlorophyll retrieval by Gitelson et al. (2006) is applied on the simulated spectra to analyse the effects of canopy structure on the pigment retrieval. The second part investigates crop land in Eschikon representing a homogeneous canopy as the next level of complexity. After an overview of the distributions of DASF values, in situ measurements of structural parameters are compared with retrieved DASF, p_1 and R. The separation of crop types in the spectral invariant space, using the two dimensions of macro and micro structure, is tested as well. In the third part, the concept of spectral invariants is further applied on a heterogeneous canopy, the forest of Lägeren, with a similar procedure. First, distributions of DASF values are examined for the whole forest. Retrieved DASF values are then compared to LiDAR retrieved structural parameters to test for sensitivities. As for the homogeneous canopy, a separation of canopy structure types in the spectral invariant space is tested in the end. After the evaluation of the usability of retrieved structural variables from hyperspectral data using the theory of spectral invariants, a method for the retrieval of plant traits is attempted. It uses the relationship of Lewis & Disney (2007) who relate biochemical constituent concentrations at leaf level to reflectance measurements through the DASF and recollision probability.

2. Data

2.1 Simulated data

In order to analyse sensitivities of the three retrieved structural parameters to leaf biochemical constituents and structural variables of an ideal canopy, simulated spectra from the version 5 PROSAIL model (Baret et al., 1992) are used. This allows to test the consistency of the retrieval and its assumptions on scenes representing ideal conditions and a perfectly homogeneous canopy. For the analysis, one parameter at a time is varied while the others are fixed to a basic parameter setting. The basic parameter setting for all spectra is given by table 1.

Table 2 contains the variations of the parameters used for the analysis. Each of the simulated spectra is then used to calculate the slope, the intercept and the R^2 of the linear fit of the retrieval as well as the DASF value (section 3.1.2).

2.2 Observational data

The hyperspectral data was recorded by the pushbroom imaging spectrometer Airborne Prism Experiment (APEX) (Itten et al., 2008) at 284 spectral bands between 399.34nm and 2420.25nm. The homogeneous canopy consisting of agricultural crop land in the area of Eschikon (Switzerland) was

Table 1. Basic parameter setting for the spectra of the PROSAIL model.

PROSPECT:		SAIL:	
Structure parameter:	1.5	Leaf area index:	3.5 m/m
Chlorophyll content (a+b):	50.0 µg/m^2	Average leaf angle:	25°
Equivalent water thickness:	0.025 cm	Hot spot:	0.05
Dry matter:	0.008 g/cm^2	Diffuse fraction:	0.15
		Sun zenith:	10°
		Relative azimuth:	0°
		View angle:	0°

Table 2. Parameter setting of the PROSAIL model for the sensitivity analysis of retrieved structural parameters to leaf biochemical constituents.

Structure parameter []	1.2	1.4	1.6	1.8	2.0	2.2	2.4	2.6	2.8				
Chlorophyll content [µg/m^2]	10	20	30	40	50	60	70	80	90				
Equivalent water thickness [cm]	0.005	0.010	0.015	0.020	0.025	0.030	0.035	0.040	0.045				
Dry matter content [g/cm^2]	0.004	0.006	0.008	0.010	0.012	0.014	0.016	0.018					
Leaf area index []	1.0	1.5	2.0	2.5	3.0	3.5	4.0	4.5	5.0	5.5	6.0	6.5	
Average leaf angle [°]	0	5	10	15	20	25	30	35	40	45	50	55	60
Sun zenith [°]	0	5	10	15	20	25	30	35	40	45			
Viewing angle [°]	0	5	10	15	20	25	30	35	40	45			

flown over on August 30, 2013, while the heterogeneous canopy of the Lägern forest area (Switzerland) area was recorded on June 29, 2010. Both datasets were radiometrically calibrated (Hueni et al., 2013), atmospherically corrected by ATCOR4 (Richter & Schläpfer, 2004) and geocoded by PARGE (Schläpfer et al., 1998), resulting in a spatial resolution of 2m. For the topographic divert area of the Lägern forest, a LiDAR derived digital surface model was used for the geocoding.

2.3 In situ retrieved structural parameters

The five in situ retrieved structural parameters for sensitivity analyses of the structural parameters retrieved from spectral data were measured in the area surrounding the ETH research station in Eschikon during the same date as the APEX overflight (Liebisch et al., 2014). They consist of integrated measurements of a 2x2m plot of the LAI, sky fraction, mean tilt angle of leaves, canopy height and destructively measured LAI. The LAI, sky fraction and mean tilt angle were all measured with the LAI 2200 Plant Canopy Analyzer (LI-COR, Inc., Lincoln, NE, USA) using a 270° view restricting cap. For the canopy height, the highest point of five random plants within the plot was measured from the ground without stretching them to their maximum length. The second LAI measurement was performed using a destructive method.

2.4 LiDAR derived structural parameters

Two LiDAR datasets are used to examine the sensitivity of retrieved structural parameters from spectral data as further independent measurements. The two datasets of structural parameters were derived from data of a full-waveform small-footprint airborne laser scanner (ALS) on August 1, 2010 under leaf-on conditions of the Lägern forest area. The footprint diameter was approximately 0.25m and a mean point density of $40m^{-1}$ was obtained.

For the first parameter set, the resulting point cloud has been subdivided into a two dimensional grid with 2m resolution in the horizontal plane (600x478m) and different structural parameters have been derived on grid basis. Following parameters were used in the analysis: vegetation height (maximum echo height above ground), vegetation length (amount of histogram bins (1m) with a percentage proportion of echoes larger than 1% in the vegetation column), vegetation ratio (vegetation length/vegetation height), crown ration (crown base/vegetation height), cumulative intensity above 3m from ground, cumulative top intensity (intensity of top 3m of canopy), height percentiles (height above ground where 10%, 20%,.., 90% and 99% of the points are located underneath) and the point density per vertical bin (always 10 bins per vegetation column).

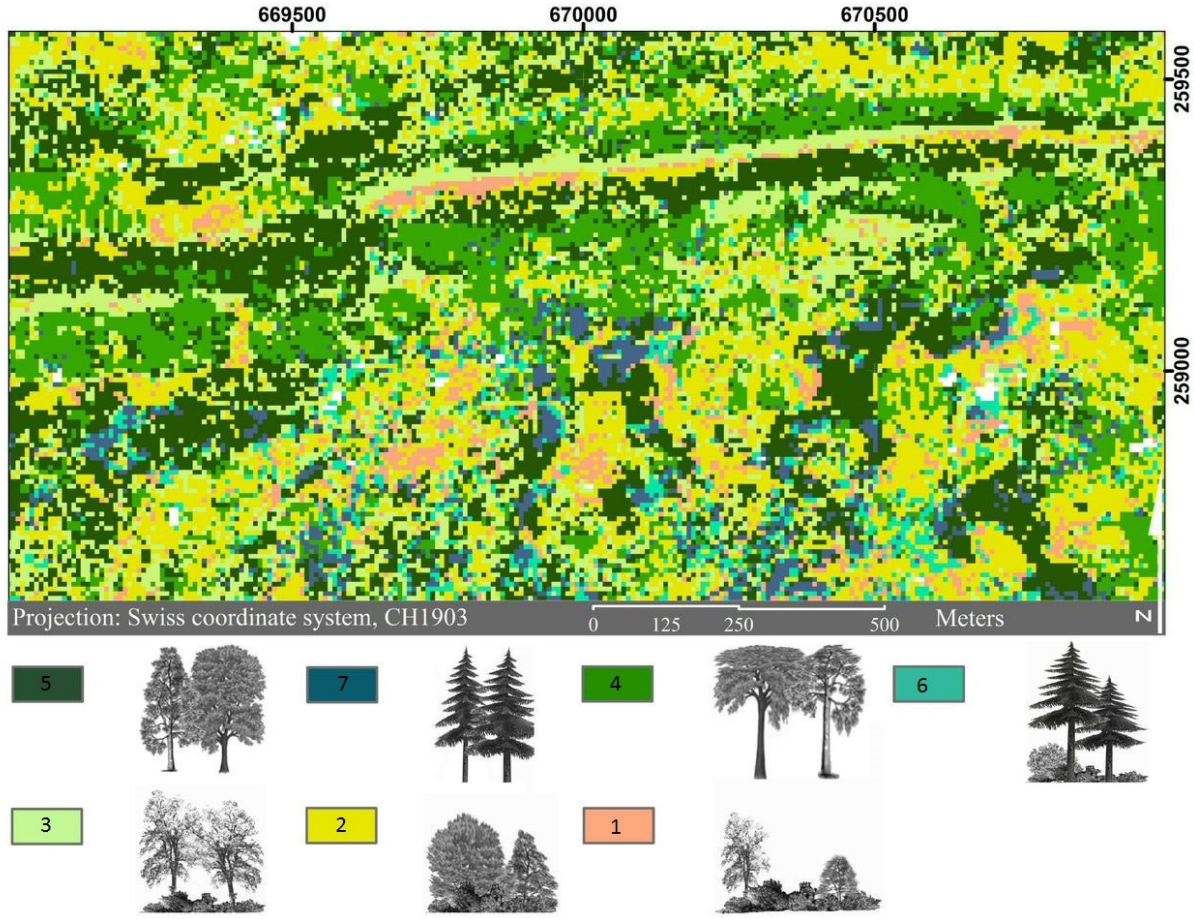

Figure 1. Canopy structure type distribution over the forest of Lägern (Leiterer et al., 2013).

The second set of ALS derived parameter consists of a three dimensional voxel grid (2400x6600x436m, 2x2x2m resolution) of the Plant Area Density (PAD) (Schneider et al., 2014). This quantity is directly derived from the point cloud of the Plant Area Index (PAI). The PAI is an estimate of all light blocking elements within a canopy and is a widely used method to describe the amount of foliage (Holst et al., 2004). Solar radiation penetrates only a few meters into dense canopy. Therefore, it is sufficient to compare the retrieved structural parameters with the highest two voxel grids since deeper structure is probably not influencing the structural parameters anymore.

2.5 Canopy structure types

For the application of the spectral invariant space for canopy type discrimination on the heterogeneous canopy of the Lägern forest, an ALS derived Canopy Structure Type (CST) was used to compare with the results of the application. The underlying ALS raw data was again the same as for

the other two LiDAR datasets. For an area of 6592x2400m (8m resolution), a classification into seven canopy structure types was performed. The result is shown in figure 1. For more details on the determination of CSTs see Leiterer et al. (2015).

3. Methods

3.1 Structural variable retrieval

3.1.1 Theory of spectral invariants

In the following section and throughout the thesis, the nomenclature of (Huang et al., 2007) is used.

Since the scattering elements (leaves) of the medium (canopy) are much larger than the wavelength of the incoming radiation, one can use geometrical optics for the radiative transfer of solar radiation through a canopy (Huang et al., 2007). The theory of spectral invariants is further based on the assumption that the canopy is bounded by a non-reflecting surface from below (Huang et al., 2007), meaning the background reflection is negligible. This assumption is valid for a dense canopy.

Solar radiation flux incident on the canopy can be split into three components: canopy transmittance t(λ), reflectance r(λ) and absorptance a(λ) (Huang et al., 2007). The canopy transmittance is the ratio of the mean downward radiation flux density at the bottom of the canopy to the downward radiation flux density above the canopy. The canopy reflectance and absorptance are defined analogous with the reflectance being the portion of the mean upward radiation flux density at the top of the canopy and the absorption being the portion of incident radiation absorbed by the canopy. According to the law of shortwave energy conservation the three components sum up to one (Smolander & Stenberg, 2005):

$$\mathrm{t}(\lambda) + \mathrm{r}(\lambda) + \mathrm{a}(\lambda) = 1 \qquad (1)$$

Similar definitions can be made on the leaf scale. The leaf transmittance and reflectance are the portions of the radiation flux density incident on the leaf that transmits through and is reflected by the leaf respectively. The leaf albedo is the sum of these two and is dependent on the leaf biochemical constituents as well as the leaf structure:

$$\omega(\lambda) = \rho_{\mathrm{L}}(\lambda) + \tau_{\mathrm{L}}(\lambda) \qquad (2)$$

Starting from these quantities a set of parameters can further be deduced. The canopy interaction coefficient, i(λ), is the mean number of interactions a photon undergoes in the canopy at a certain wavelength (Huang et al., 2007). It is the ratio of the canopy absorptance to the mean absorptance of a leaf (Knyazikhin et al. , 2005):

$$\mathrm{i}(\lambda) = \frac{\mathrm{a}(\lambda)}{\mathrm{a}-\omega(\lambda)} \qquad (3)$$

By multiplying the canopy interaction coefficient with the leaf albedo, one gets the portion of photons scattered by leaves, $\omega(\lambda)\cdot i(\lambda)$. According to (Smolander & Stenberg, 2005) the canopy interceptance i_0 is the probability that a photon from the incident radiation will hit a phytoelement ($\omega(\lambda) = 0$).

Huang et al., (2007) further illustrate that the difference between portions of photons incident on scattering elements at two different wavelengths, $i(\lambda) - i(\lambda_0)$, is proportional to the difference between portions of photons scattered by scattering elements at the same wavelengths, $\omega(\lambda)i(\lambda) - \omega(\lambda_0)i(\lambda_0)$. The ratio of both terms, a combination of basic quantities from radiative transfer, therefore loses any dependency on wavelength and is an example for a spectrally invariant parameter:

$$p = \frac{i(\lambda)-i(\lambda_0)}{\omega(\lambda)i(\lambda)-\omega(\lambda_0)i(\lambda_0)} \tag{4}$$

p is named the recollision probability (Stenberg, 2007) and is the probability that a photon scattered by a scattering element will interact again within the canopy (Knyazikhin et al., 2005; Panferov et al., 2001; Smolander & Stenberg, 2005). It is largely insensitive to the direction of the incident beam and therefore an intrinsic canopy property (Huang et al., 2007).

As deduced by (Knyazikhin et al., 2013), a photon incident on the canopy can be intercepted by the foliage with a probability of i_0 or pass through the canopy without any interaction. If it gets intercepted by the foliage, the photon can either be absorbed or scattered by a phytoelement. The absorption and scattering is determined by the leaf albedo ω_λ and is wavelength dependent. If the photon is scattered it can further either recollide with a phytoelement with a probability p or exit the canopy. If it exits the canopy with a probability of (1-p) the photon can get registered by the sensor with a probability $\rho(\Omega)$, where Ω is the direction between the scattering location and the sensor. $\rho(\Omega)$ is called the directional gap density (Knyazikhin et al., 2013). The parameters i_0, p and $\rho(\Omega)$ are all wavelength independent and only a function of the canopy structure and viewing geometry. They can be combined into the directional area scattering factor (DASF):

$$\mathrm{DASF} = \rho(\Omega)\frac{i_0}{1-p} \tag{5}$$

Further, the bidirectional reflectance factor (BRF) can be approximated by the quantities of the DASF and the leaf albedo if the assumptions for the spectral invariants theory are respected:

$$\mathrm{BRF}_\lambda(\Omega) = \rho(\Omega)\frac{i_0}{1-\omega_\lambda p}\omega_\lambda \tag{6}$$

However, as stated by Lewis & Disney, (2007) it is not possible to partition the canopy signal into its structural and leaf biochemical constituents as long as either of both is known, which is not the general case in remote sensing.

In the spectral interval between 710 – 790nm the radiation scattered from the leaf interior is principally controlled by the absorption characteristics of chlorophyll, dry matter and water (Knyazikhin et al., 2013). Furthermore, theoretical and empirical studies (e. g. Lewis & Disney, 2007; Schull et al., 2011) have found that transformed spectra can be related to a fixed spectrum through spectral invariant relationship in the same spectral interval:

$$\overline{\omega}_\lambda = \frac{1-p_L}{1-p_L\overline{\omega}_{0\lambda}}\overline{\omega}_{0\lambda} \tag{7}$$

Here, $\overline{\omega}_{0\lambda}$ is the fixed reference spectrum and p_L is the within-leaf recollision probability. The transformed spectrum corresponds to the fraction of radiation scattered from the leaf interior that interacted with the leaf constituents only. Radiation coming from the leaf interior is dominant in the spectral interval between 710nm and 790nm for which reason radiation scattered from the leaf surface can be neglected, and following assumption is valid for this interval (Knyazikhin et al., 2013):

$$\omega_\lambda \approx i_L\overline{\omega}_\lambda = \frac{1-p_L}{1-p_L\overline{\omega}_{0\lambda}} i_L\overline{\omega}_{0\lambda} \tag{8}$$

, where i_L is the leaf interceptance (fraction of radiation incident on the leaf that enters the leaf interior). This expression for the leaf albedo can be substituted into equation (6):

$$BRF_\lambda(\Omega) = \frac{i_0\rho(\Omega)(1-p_L)i_0}{1-\overline{\omega}_{0\lambda}p_1}\overline{\omega}_{0\lambda} \tag{9}$$

where p_1 is:

$$p_1 = p_L + i_L p(1-p_L) \tag{10}$$

and corresponds to the overall recollision probability of Lewis & Disney (2007). p_1 is a combined recollision probability that considers the impact of multiple scales of scattering (Lewis & Disney, 2007). By rearranging equation (9), one obtains a linear relationship between BRF/$\overline{\omega}_{0\lambda}$ and BRF in the interval 710 – 790nm:

$$\frac{BRF_\lambda(\Omega)}{\overline{\omega}_{0\lambda}} = p_1 BRF_\lambda(\Omega) + i_L\rho(\Omega)(1-p_L)i_0 \tag{11}$$

The slope p_1 and intercept R = $i_L\rho(\Omega)(1-p_L)i_0$, both spectrally invariant and mostly characteristics of the canopy structure, therefore determine the relationship between a fixed spectrum and the BRF

of the given canopy. R is the escape probability along a given direction termed the directional escape probability (Knyazikhin, 2013). The ratio $R/(1 - p_1)$ furthermore gives the DASF in the form:

$$\mathrm{DASF} = \rho(\Omega)\frac{i_0 i_L}{1-p} \tag{12}$$

Equation (6) once again can be rearranged and simplified as shown by Knyazikhin et al. (2013):

$$\mathrm{BRF}_\lambda(\Omega) = \mathrm{DASF} \cdot W_\lambda \tag{13}$$

, where W_λ is the canopy scattering coefficient:

$$W_\lambda = \frac{1-i_L p}{1-i_L p\hat{\omega}_\lambda}\hat{\omega}_\lambda \tag{14}$$

and $\hat{\omega} = \omega_\lambda/i_L = \overline{\omega}_\lambda + s_L/i_L$. The canopy scattering coefficient can thus be approximated by the ratio BRF/DASF, however, not accounting for surface properties of the leaves (i_L) (Knyazikhin et al., 2013). Therefore, the DASF is a factor that corrects spectral data for canopy structural effects.

Through the investigation of the impacts of the recollision probability over different spatial scales (leaf to canopy level), Lewis & Disney (2007) work out an equation that relates the canopy scattering coefficient via the recollision probability to the leaf biochemical constituents:

$$\sum_{i=1}^{i=m} C_i k'_i(\lambda, n) = -\ln\left[\frac{W(\lambda)}{1-p_1(1-W(\lambda))}\right] \tag{15}$$

In equation (15), C_i is the concentration of the leaf biochemical constituent i and $k'_i(\lambda, n)$ the specific absorption coefficient of the same constituent, which is dependent on wavelength and refractive index, n, of the leaf surface. Lewis & Disney (2007) show that the impacts of n and p_L (contained in p_1) are rather small.

Furthermore, the spectral invariant space enables to discriminate crop and canopy structure types according to the two dimensions of the macro and micro structure of canopies. The natural logarithm of the ratio of the intercept to the total escape probability, ln[R/(1-p)], is related to the macro structure of the canopy, e.g. tree spatial distribution, crown geometry and crown transparency. ln(1-p) in contrast is related to the number of hierarchical levels within a pixel and characteristics like leaf distribution and leaf density. Since crop or tree types exhibit differences in both structural dimensions, the position in the spectral invariant space allows the separation or even classification of them. (Carmona et al., 2009; Knyazikhin et al., 2009; Schull et al., 2011)

3.1.2 Application of the theory of spectral invariants - Retrieval of structural parameters

The DASF retrieval used in this thesis follows the algorithm proposed by Knyazikhin et al., (2013). The reference spectrum required by the retrieval is simulated with PROSPECT (Jacquemoud & Baret, 1990) and the following input parameters:

Structure parameter: 1.5
Chlorophyll content: 16.0 µg/cm^2
Carotenoid content: 10.0 µg/cm^2
Brown pigments: 0.0 µg/cm^2
Equivalent water thickness: 0.005 cm
Leaf mass: 0.002 g/cm^2

The reference spectrum is then taken as the sum of the simulated reflection and transmission. For each pixel a linear relationship between the reflectance data and the reflectance data divided by the reference spectrum is fitted for the region between 710nm and 790 nm (equation (11)). The slope, p_1, the intercept, R, the goodness of the linear fit, R^2 and the DASF value are all written to a separate layer of a new file. It is important to emphasise the difference between the recollision probability, p, and the slope, p_1. Latter corresponds to the overall recollision probability and includes the within leaf recollision probability, p_L, (formula (10)). This is important insofar as the retrieval of structural parameters permits to retrieve the overall recollision probability only. Therefore, the retrieved and analysed overall recollision probability is expected to show also sensitivities to leaf biochemical constituents beneath sensitivities to structural related parameters, which is not the case for the spectral invariant recollision probability. The sensitivity to leaf biochemical constituents is also valid for R. The retrieval of structural parameters is performed in the raw viewing geometry for pure radiometry and transformed geometrically thereafter. As a next step all pixels with a R^2 smaller than

Table 3. Spectral bands for retrieving pigment content from leaf reflectance spectra (Gitelson et al., 2006)

	λ_1 [nm]	λ_2 [nm]	λ_3 [nm]
Chlorophyll	690 - 725	760 - 800	760 - 800
Carotenoids	510 - 520	690 - 710	760 - 800
Anthocyanin	540 - 560	690 - 710	760 - 800

a threshold value are filtered out in order to only use pixels were the theory of spectral invariants is valid. This value is elaborated for each of the two scenes by interactive manual investigation of the true colour images and corresponding R^2 layers. For the heterogeneous canopy scene a further filtering is applied to remove shadowed pixels due to the illumination geometry. Thus, a threshold value in band 66 (727.9 nm) of the APEX sensor is determined visually by comparison with the true colour image of the scene.

3.2 Retrieval of pigments and leaf biochemical constituents

One method to derive leaf pigment concentration is presented by Gitelson et al. (2006), who build up their simple three-band model on the conceptual model developed by Gitelson et al. (2003):

$$[\mathrm{R}(\lambda_1)^{-1} - \mathrm{R}(\lambda_2)^{-1}] \cdot \mathrm{R}(\lambda_3)^{-1} \propto \mathrm{C_i} \qquad (16)$$

They find three spectral bands ($\lambda_{1\text{-}3}$; table 3) for each of chlorophyll, carotenoids and anthocyanin that fit into the model and show high correlations with extracted pigment concentrations, C_i, of the respective pigments. However, this method is elaborated for leaf level reflectance only where structural effects are not accounted. The application of this model on remote sensing data of vegetation would therefore lack in a correction for structural effects resulting in biased concentrations.

A possible solution to incorporate structural effects in the estimation of leaf biochemical content from hyperspectral data is tested here with the implementation of equation (15). This equation is derived by Lewis & Disney (2007). As described in the theory section, it links leaf biochemical constituent concentrations to reflectance measurements, accounting for canopy structure. The equation contains following variables: reflection, DASF and recollition probability of a pixel, the absorption coefficients (figure 14a) and the concentrations of leaf biochemical constituents. The right hand side of the equation comprises of the reflection and the structural variables, which equals the superposition of the effective absorption of each leaf constituent (left hand side). It is hypothesised that one should be able to solve for the concentration of each constituent, if enough spectral bands are available. Contrariwise, Lewis & Disney (2007) also postulate the impossibility to derive both, structural parameters and leaf biochemical concentrations at the same time from hyperspectral data. By bringing in the retrieval of structural parameters, however, a new variable is added to the problem in the form of the reference spectrum. Through the relationship of BRF/$\overline{\omega}_0$ and BRF, the

two needed structural variables can be retrieved. The retrieved variables (DASF and p_1) can then be inserted in equation (15) together with the reflectance and known specific absorptions, which leaves only the leaf biochemical concentrations unknown.

The method for the retrieval of leaf biochemical concentrations is chosen utilising a look up table (LUT). First, the LUT is generated to simulate the absorption spectrum of a leaf (left hand side of equation (15)) using the constituent concentration, specific absorption coefficients of the structural parameter, chlorophyll a+b, carotenoid, dry matter and the equivalent water thickness and a refractive index, n, of 1.4 as proposed by Lewis & Disney (2007). The absorption spectra of all possible combinations of constituent concentrations (table 4) are saved in the LUT with a spectral resolution of 1 nm.

In a second step, the right hand side of equation (15) is calculated. The reflectance data from APEX is corrected with the according DASF to get the canopy scattering coefficient (equation (13)) and the negative natural logarithm of the ratio, incorporating the recollision probability, is calculated. Next, the LUT has to be convoluted to the wavelengths of the APEX sensor. The last step compares the retrieved absorption spectrum of each pixel with the ones of the LUT and assigns the root mean squared error for each comparison. The combination of constituent concentrations of the LUT with the smallest error should therefore come closest to the one of the pixel.

Table 4. Biochemical constituent concentrations used for the simulated absorption spectra of the look up table.

Structure parameter []	1.6	1.8	2.0	2.2	2.4				
Chlorophyll content [µg/m^2]	30	35	40	45	50	55	60	65	70
Carotenoid content [µg/m^2]	2	4	6	8	10				
Equivalent water thickness [cm]	0.015	0.020	0.025	0.030	0.035				
Dry matter content [g/cm^2]	0.008	0.010	0.012	0.014	0.016				

3.3 Simulated reflectance data

3.3.1 Sensitivity analysis of retrieved structural parameters to parameter variation of the model

First, the effects of the variation of different model parameters (table 2) to the DASF are plotted, analysed and compared to similar results of the literature. The intent is to evaluate the coherence of sensitivities experienced by the DASF. However, different effects could be blurred when considering only the DASF. For a more detailed evaluation of the coherence of the retrieval, variations of the model parameters are further compared to the resulting overall recollision probability, p_1, and directional escape probability, R. The attribution to geometrical and structural parameters is simpler for these retrieved parameters as they can further be related to more concrete parameters, e. g. LAI, viewing angle or gap fraction (Rautiainen et al., 2004; Smolander & Stenberg, 2005; Wang et al., 2011). Using simulated spectra is a big advantage for the analysis of structural dependencies of p_1 and R. Both are sensitive to leaf biochemical constituents as their definition contains the within leaf probability p_L. The concentrations of the biochemical constituents can be hold constant in the model, through which p_1 and R are only sensitive to structural parameters.

3.3.2 Pigment retrieval with simulated data

Lastly, the pigment retrieval of Gitelson et al. (2006) is performed for chlorophyll using the simulated spectra to examine how canopy structure influences the retrieval. The concentration of chlorophyll is first varied in the PROSPECT model (leaf spectrum only) with all the other parameters hold constant. Then the chlorophyll content is set to a constant value and the LAI is varied in the SAIL model (Verhoef, 1984). The correlation between the retrieved chlorophyll content and the chlorophyll values used in the PROSPECT model is taken as function to relate retrieved chlorophyll content for the SAIL model to “real” chlorophyll content. A linear correction of retrieved chlorophyll content with the DASF is further tested, which would represent a simple method to correct retrieved pigment concentrations for structural influences of canopies.

3.4 Observational data of homogeneous and heterogeneous canopies

The structural parameter retrieval for the data of the homogeneous canopy in Eschikon is performed before the geometrical rectification to use the pure radiometry of the data. However, both the geometrically corrected and uncorrected DASF retrieval are used depending on the available in situ data. The crop types of the different fields are given in the raw geometry, while the in situ retrieved structural measurements are given in the true geometry.

For the analysis with the two LiDAR derived parameter sets the DASF retrieval for the heterogeneous canopy of the Lägern area is performed before the geometrical rectification where the CST-dataset is not used. Since the CST-dataset is given in 8m resolution, the DASF map is resampled to the same resolution of 8m. Therefore, the DASF map is first geometrically rectified and then resampled because no geometrical data is available for the 8m resolution.

3.4.1 Distribution of DASF values

To examine whether the homogeneity of the agricultural canopy is also reflected by the DASF values, 53 fields (figure 6a) are selected via regions of interests (ROI) and assigned with crop type to compile two statistics. Out of these 53 fields, 16 are corn (co), 11 temporal grassland (tg), 11 meadow grassland (mg), 5 natural grassland (ng) and 8 sugar beet (brs). An additional crop type is created by merging the three grassland classes into grassland (g). First, all fields of one crop type are taken together to form one class. The mean and standard deviation of the DASF values are compared between the classes to analyse how the different crop types differ from each other in respect to the DASF. In a second step the mean DASF value and standard deviation of the different fields of one crop type are compared to each other to check how the DASF values vary within one crop type. The statistics are complemented by manual investigations of the scenes.

The first investigation of the heterogeneous canopy examines different distributions of DASF values. The starting point is the DASF statistic over the whole forest of the Lägern. Next, the distribution of DASF values between the original spatial resolution of 2m and the resampled spatial resolution of 8m is compared to check for resampling effects of the retrieval of structural parameters from hyperspectral data. Illumination effects are also analysed by comparing the DASF values of the northern side of the Lägern hill with the more exposed southern side.

3.4.2 Sensitivity analyses of retrieved structural parameters to in situ retrieved and LiDAR-derived structural parameters

Analog to the simulated data, a sensitivity analysis is conducted with the retrieved structural parameters from the remotely sensed spectral data. For the homogeneous canopy of Eschikon, in situ retrieved structural parameters (2.3) are compared to the retrieved ones (DASF, p_1 and R) and relationships are tested for coherence. Other than for the simulated spectral data, the canopies of the remotely sensed data do not experience constant leaf biochemical constituent concentrations. Competing effects to structural sensitivities are therefore expected from the biochemical constituent variability in the sensitivity analyses of the overall recollision and directional escape probabilities. The DASF, however, should not experience such sensitivities since no leaf parameter is included in its definition. The in situ measurements are given as point data with a GPS location, but are integrated measurements of a 2x2m plot. A plot of 3x3 pixels (6x6m) around the pixel containing the GPS location was selected in the scene of the retrieved structural parameters. The average of these pixels is then taken as approximation of the retrieved parameter value for the comparison with the corresponding point data of the in situ measurement.

LiDAR derived canopy structure parameters of the Lägern forest parametrise relatively distinct characteristics of the canopy structure and represent well qualified references for sensitivity analyses of the DASF. The different LiDAR derived structural parameters are therefore compared to the DASF to further test the coherence of retrieved structural parameters from spectral data of a heterogeneous canopy.

3.4.3 Crop and canopy type discrimination in the spectral invariant space

As described in 3.1.1, the spectral invariant space allows the separation of crop types or tree species. Therefore, the two dimensions of macro and micro structure are used to span the plane and the position within the plane is determined by structural characteristics of the pixel. This analysis tests if the discrimination of crop or canopy types in the spectral invariant space is possible using the retrieved parameters p_1 and R. The sensitivity to leaf biochemical constituents of p_1 and R probably interferes with the sensitivity to structural parameters, which could result in challenges regarding the coherence of the spectral invariant space.

For crop properties like crop height, crop width, ground cover and distribution are affecting the macro structure, while the number of hierarchical levels within a pixel, e.g., leaf density and leaf distribution, is in contrast related to the micro structure (Carmona et al., 2009; Knyazikhin et al.,

2009; Schull et al., 2011). The location of a point in the spectral invariant space can therefore separate crops according to their macro and/or micro structure. To generate the spectral invariant space the average values of the directional escape probability and the overall recollision probability from each of the 53 fields are taken to place the fields into the spectral invariant space. The same is also performed using the data retrieved from the plots (see 3.4.2).

Analog to the homogeneous canopy, the discrimination of canopy types is tested using the spectral invariant space. For forested areas the macro structure is related to parameters like tree spatial distribution, crown geometry and crown transparency. The micro structure on the other side is related to leaf distribution and leaf density, e.g. leaf/needle clumping, within the canopy (Schull et al., 2011). Here, a larger influence of the macro structure compared to the agricultural canopies is expected because of the different crown geometries. In addition, the differences between leaf and needles impact the micro structure as well resulting in a better differentiation of canopy types in both dimensions.

3.5 Using the theory of spectral invariants for the retrieval of leaf biochemical constituents

The retrieval of the leaf biochemical constituent concentrations from spectral measurements, which is corrected for canopy structure and presented in section 3.2 is tested on corn field number 1. Therefore, the mean values of the field are taken for the retrieved structural variables (DASF and p_1), while the retrieval is performed per pixel of the reflectance data. The reason is challenges shown later to appear while retrieving structural variables on pixel level of this resolution.

4. Results

4.1 Simulated reflectance data

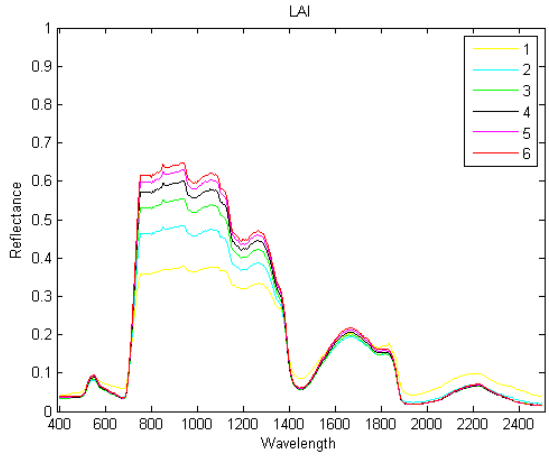

a

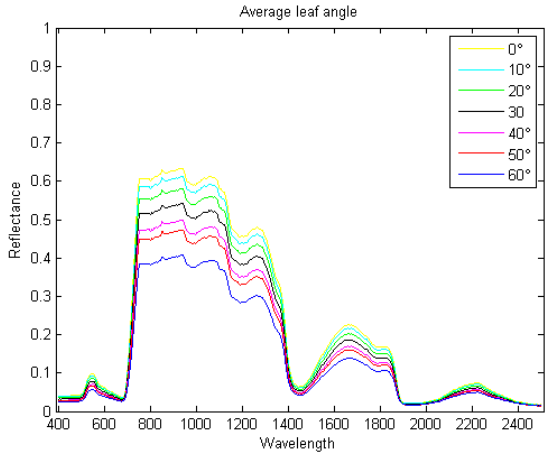

b

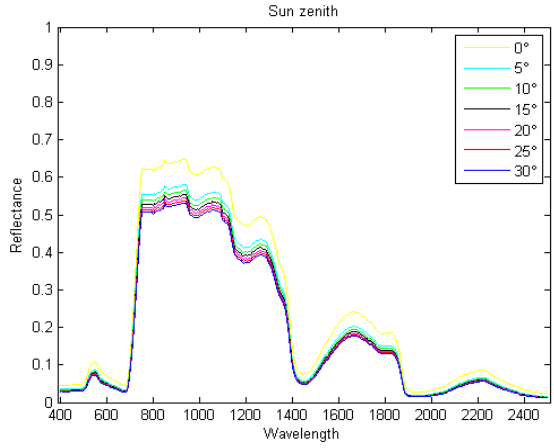

c

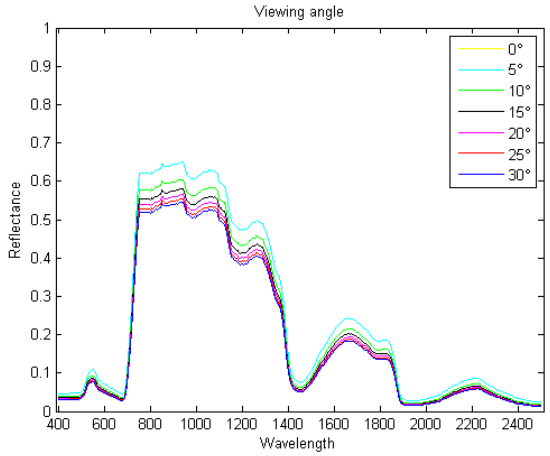

d

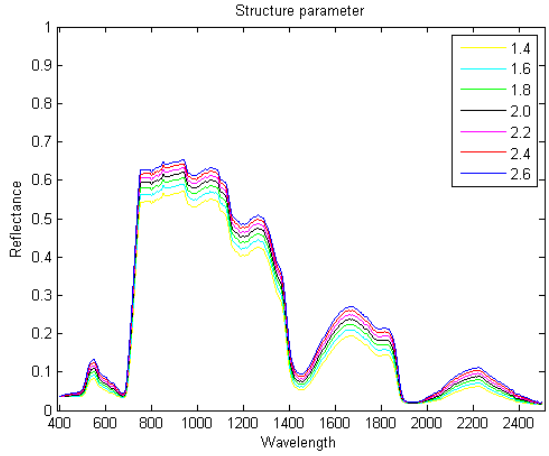

e

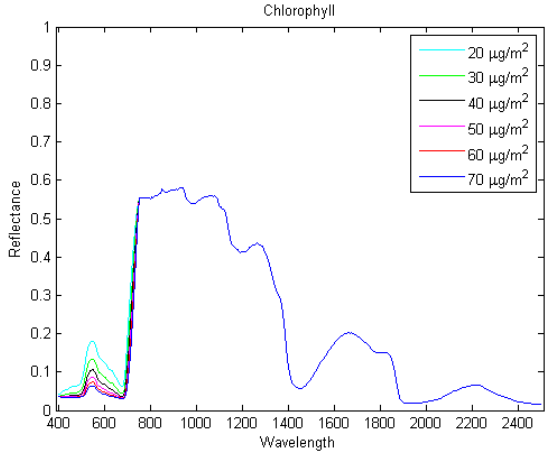

f

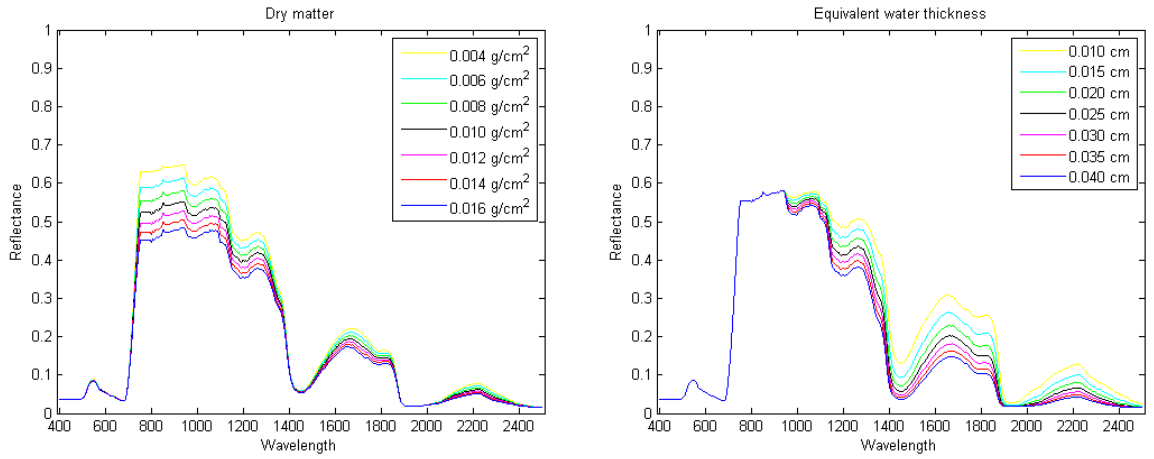

g h

Figure 2. Simulated spectra using the PROSAIL model with varying leaf biochemical and structural input parameters

The figures 2a-h illustrate a part of the PROSAIL spectra described in section 2.1 (table 1 and 2) and used in the sensitivity analysis of retrieved structural parameters of the simulation section. As expected, the spectra of the structural parameters (fig. 2a-d), the structure parameter of the leaves (fig. 2e) and the dry matter (fig. 2g) vary over the whole spectral range whereas the ones of the chlorophyll (fig. 2f) and the equivalent water thickness (fig. 2h) only vary within the characteristic spectral region of their absorption.

4.1.1 Sensitivity of DASF to parameter variation

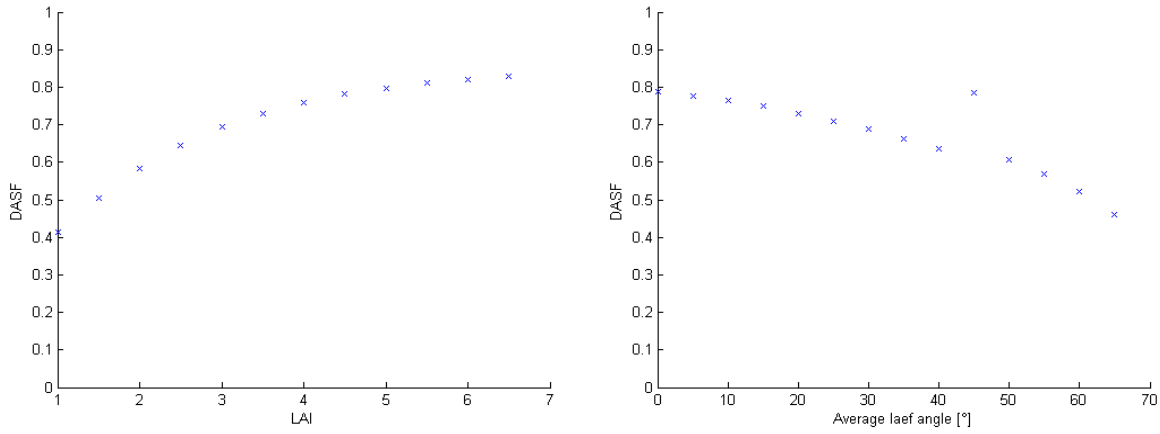

a b

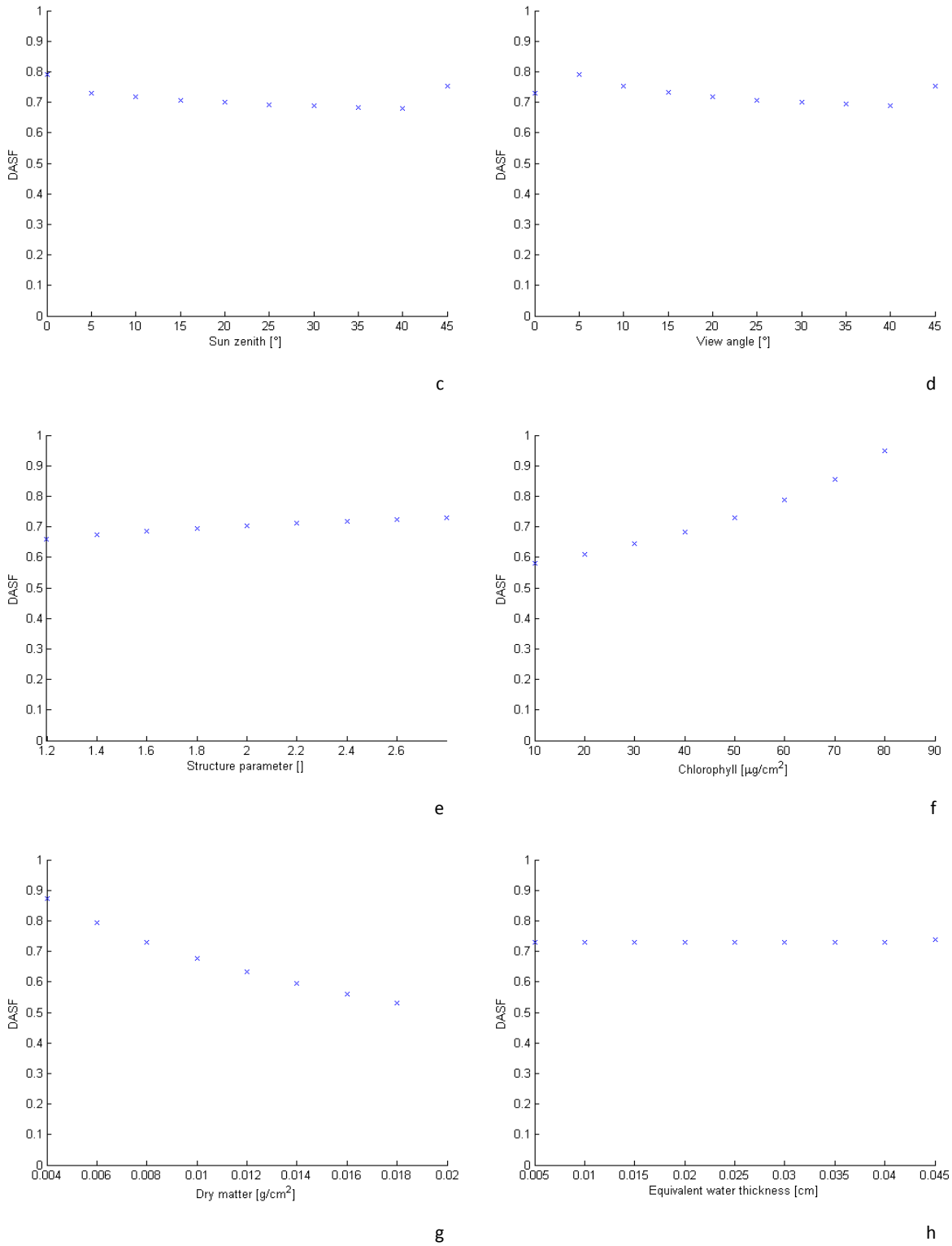

Figure 3. Sensitivity analysis comparing the retrieved DASF to input parameters of the PROSAIL model

The figures 3a-h show the variation of the DASF for the different parameter settings of the PROSAIL model.

A comparable relationship as presented by Rautiainen et al., (2009) and Mõttus (2007) between the DASF and the LAI is found here (fig. 3a) linking the DASF to a characteristic structural variable of the canopy. This relationship probably arises from a strong link between the recollision probability of a canopy and the LAI (Smolander & Stenberg, 2005) which will be analysed in the next section. The characteristic saturation effect experienced by the spectrum (fig. 2a) is furthermore also found in the DASF.

As expected, the average leaf angle of the canopy medium has a large influence on the DASF (fig. 3b). Assuming a predominantly homogeneous canopy with a uniform leaf angle distribution, a photon entering the canopy and interacting with a leaf can escape the canopy after the interaction through a gap in a certain direction (3.1.1). If the leaf distribution stays unchanged and the photon is located at the same point in the canopy as before but the leaf angle changes, the gap distribution will be different. While gaps in certain directions will be larger, others will diminish. Also, for a fixed viewing geometry in geometrical optics, a point outside the canopy will receive a different amount of reflected radiation if the reflecting surface varies its tilt angle. Therefore, the directional escape probability and consequently the DASF should theoretically vary with a varying mean tilt angle of the leaves. Latter explanation is most certainly the reason for a lower DASF with higher leaf angle. Since the viewing geometry is set to 10° sun zenith and 0° viewing angle, a higher leaf angle scatters more radiation in a flat angle. Therefore, less radiation reaches the sensor. In addition, the scattered radiation travels a longer way through the vegetation when scattered in a flat angle which results in a higher absorption probability (Smolander & Stenberg, 2005). The outlier at 45° on the other side is very surprising and cannot be explained. The much higher DASF compared to the surrounding values is indicative of a smaller influence of the structure for this leaf angle. However, as described above, more radiation is scattered away for larger leaf angles. Also, this angle is far from resulting in a hot spot effect with a viewing angle of 0° and sun zenith of 10°. Another effect not clear here seems to play a major role for this leaf angle, thus.

After a steeper jump downward of the DASF value between the sun zenith angles of 0° and 5° (fig. 3c), the DASF values are only decreasing slowly with sun zenith angle. These findings seem in line with Knyazikhin et al. (2013), who report that the canopy interceptance is depending on the solar direction, but is approximately unity for dense vegetation. The next section will show whether this relationship is also supported for the present data. Again very surprising, the sun zenith angle of 45° looks like an outlier. Comparing the results with the ones from (Adams, 2013), however, suggests that this outlier is more an artefact of the data range. The findings from Adams (2013) show that the DASF values, after decreasing until 45°, start to increase again for larger sun zenith angles. Therefore,

the findings presented here seem to support the ones from Adams (2013). It must be noted, though, that there is less variation in the DASF here than there is in the results of Adams (2013).

The of the DASF to viewing angle is similar to the one of the sun zenith angle, however, the steep jump between 0° and 5° viewing angle being upward (fig. 3d). The outlier at 45° can, again, be explained with the findings of Adams (2013), who's relationship between the DASF and the viewing angle is similar to a quadratic function. On the other side, while the DASF is very slightly increasing between 0° and 45° in her analysis, figure 3d here suggests a different progression of the DASF with viewing angle. This could be due to different setups of simulated canopies.

Figures 3e-h illustrate very surprising results. While the DASF is nearly not sensitive to the equivalent water thickness (fig. 3h) the concentrations of the other biochemical constituents affect the DASF clearly, although the canopy structure parameters of the model are hold constant. Contrary to its definition, the DASF retrieved in this analysis is sensitive to biochemical constituents, especially chlorophyll and dry matter content. The DASF values vary between 0.64-0.78 (fig. 3f) and 0.73-0.59 (fig. 3g) for rather normal chlorophyll and dry matter contents of 30-60 µg/cm^2 and 0.008-0.014 g/cm^2 respectively. The reason for the sensitivity to different concentrations of biochemical constituents, at least in this analysis, is apparent when looking at the spectra; the most obvious two being the ones of dry matter and chlorophyll (fig. 2f and g). The variation of the reflectance for the fixed parameter set and varying dry matter concentration is weak around 710nm. Nearly no difference in the reflectance spectrum is therefore apparent for the different dry matter concentrations around the wavelength 710nm. Around 790nm, however, the spectrum varies much more for different dry matter concentrations of the model (fig. 2g). Chlorophyll shows a comparable picture, but with the reflectance around 710nm being the shifting one while the reflectance around 790nm is constant for all concentrations (fig. 2f). The resulting behaviour of the spectrum for both biochemical constituent variations is that the slopes between 710nm and 790nm of the spectra differ strongly from each other. When calculating the DASF, this part of the spectrum is used to fit the linear relationship between HCRF/$\omega 0_\lambda$ vs. HCRF. Since the function of the HCRF spectrum, which differs between the constituent concentrations, is always normalised by the same function of $\omega_{0\lambda}$, the function HCRF/$\omega_{0\lambda}$ vs. HCRF consequently varies between the constituent concentrations as well. Therefore, the slope and the intercept of latter function vary too, resulting in a sensitivity of the DASF to different leaf biochemical constituent concentrations (fig. 3f and 3g). This effect is also apparent for the structure factor (fig. 2e and 3e), however, not for the equivalent water thickness (fig. 2h and 3h) since water is not absorbing in this spectral range.

4.1.2 Sensitivity of overall recollision and directional escape probabilities to parameter variation

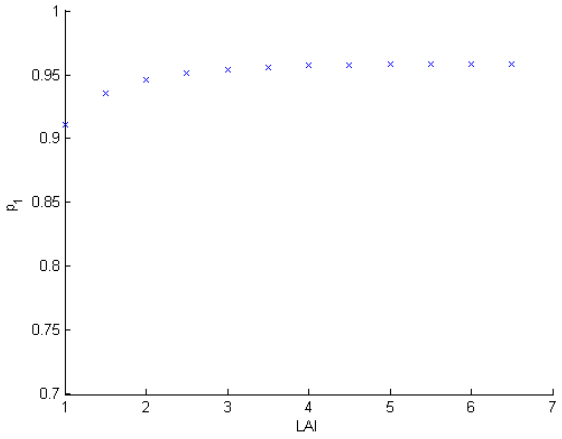

a

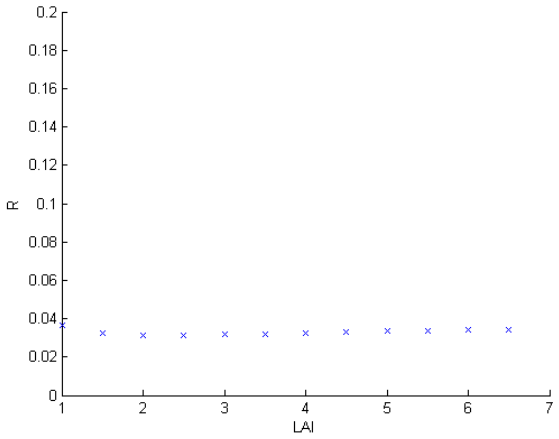

b

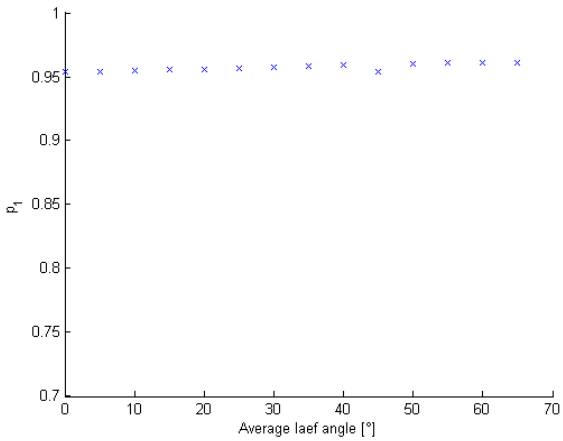

c

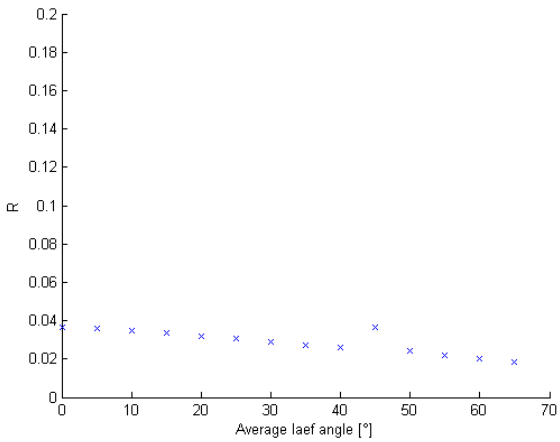

d

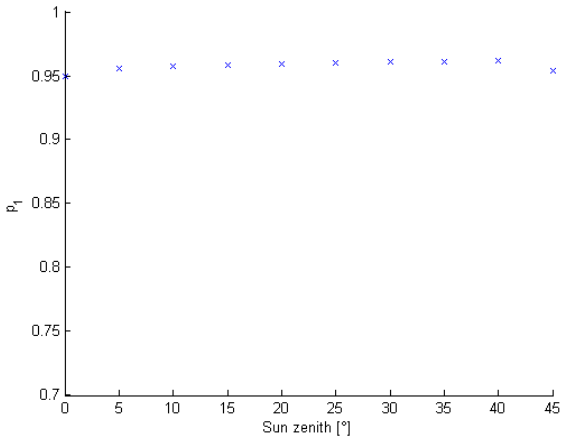

e

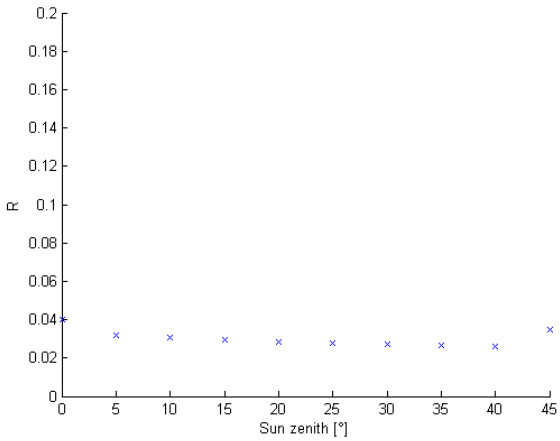

f

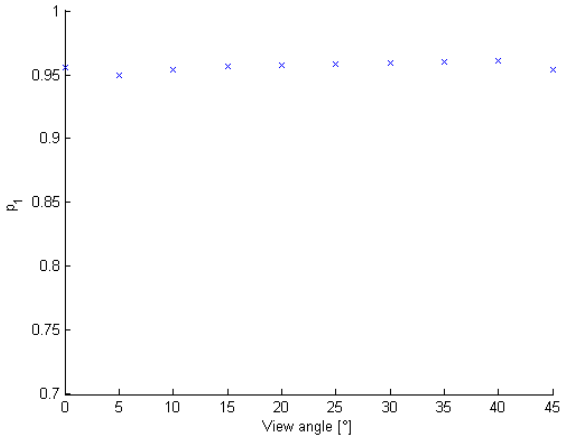
ρ_1
View angle [°]

g

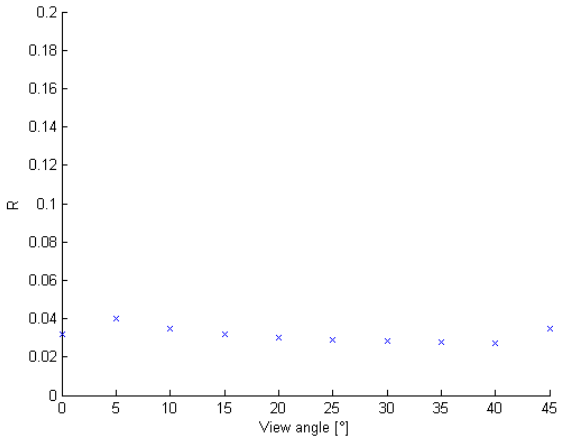
R
View angle [°]

h

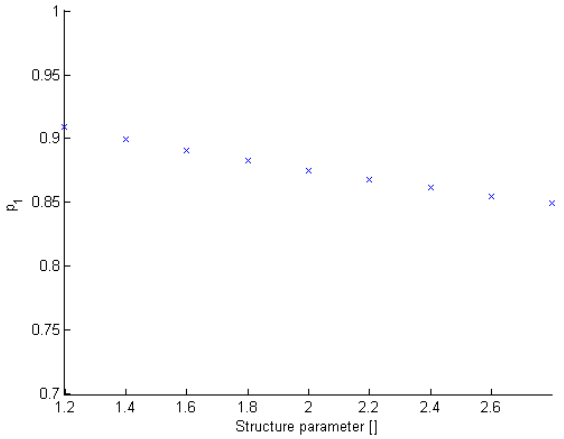
ρ_1
Structure parameter []

i

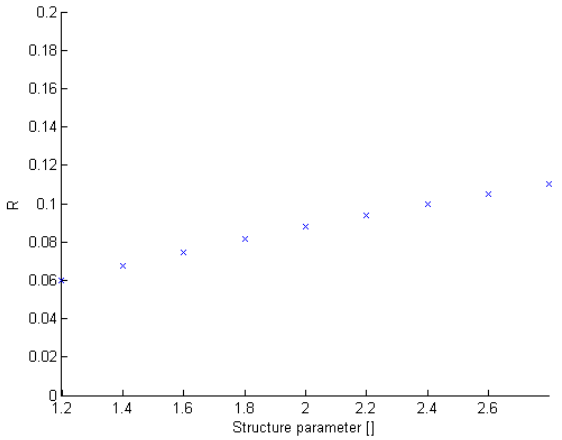
R
Structure parameter []

j

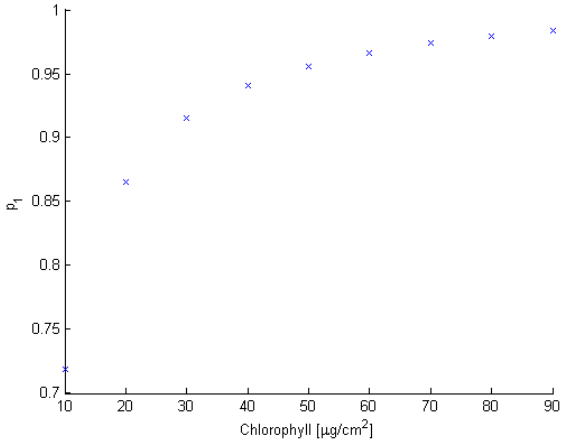
ρ_1
Chlorophyll [µg/cm^2]

k

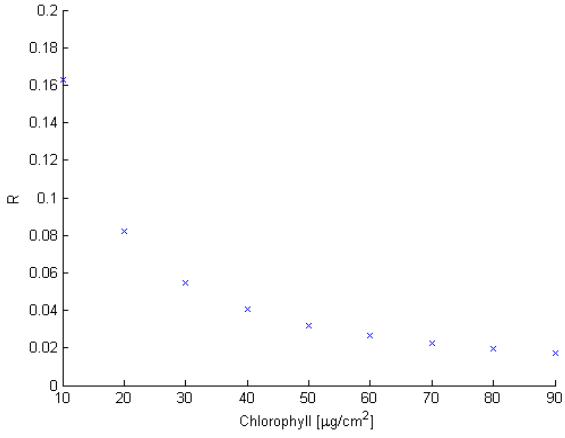
R
Chlorophyll [µg/cm^2]

l

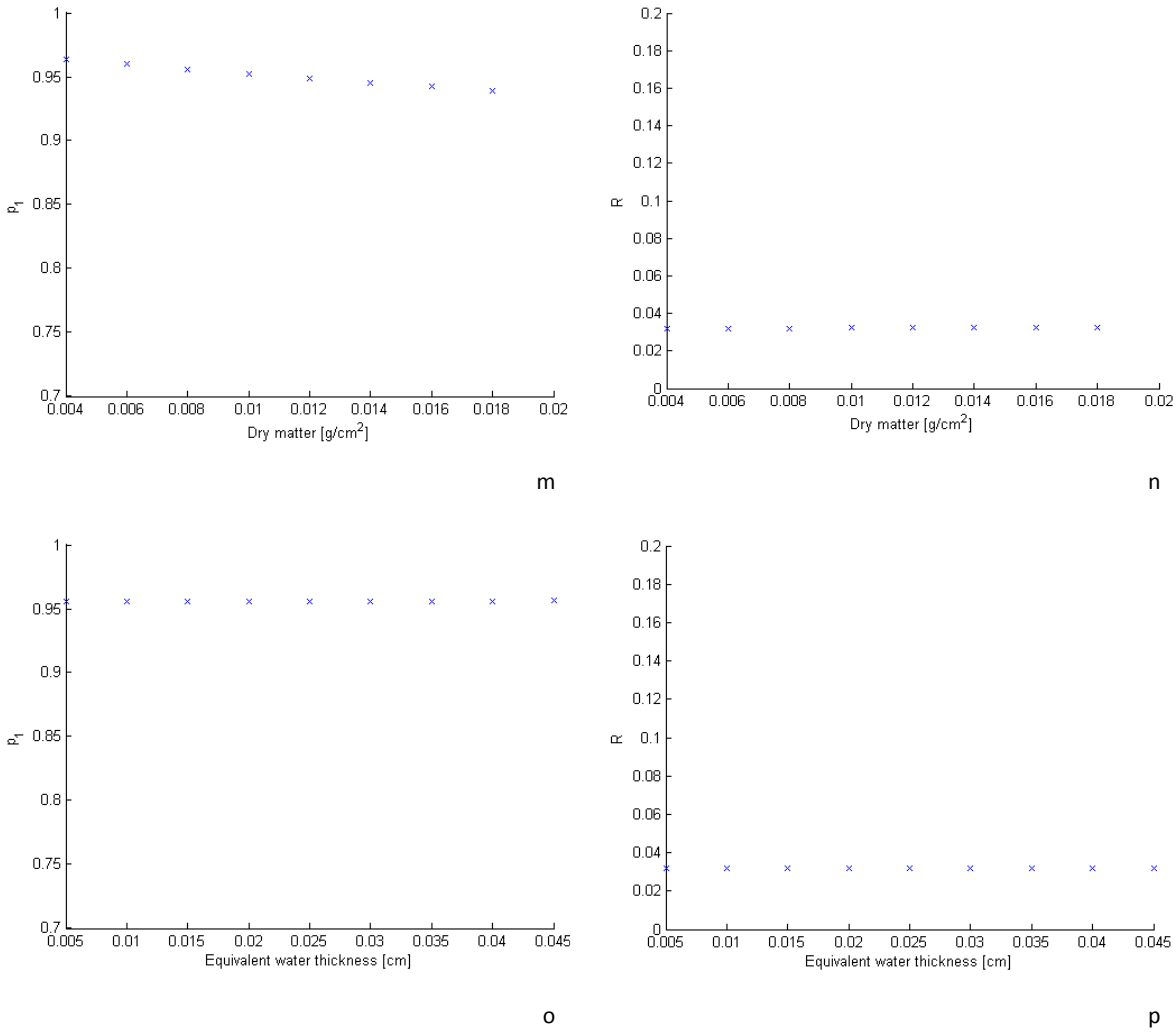

Figure 4. Sensitivity analysis comparing the overall recollision and directional escape probabilities to input parameters from the PROSAIL model

The figures 4a and b show the expected results with the characteristic saturating relationship between p_1 and the LAI and no correlation between the LAI and R. Compared with the studies of Rautiainen et al., (2009) and Mõttus (2007) however, the range of p_1 is much smaller and the curve flattens already for lower LAIs. This could be due to the perfectly distributed scattering elements of the canopy that result in higher overall recollision probabilities compared with real canopies of small LAIs.

The results for the average leaf angle (fig. 4c and d) follow, again, the expectations. p_1 shows a very small positive trend but the variation is probably negligible and can therefore be assumed constant compared with R. The sensitivity of R to the average leaf angle strengthens the argumentation of the last section that the directional escape probability is reduced for larger leaf angles. Reflectance from a canopy with larger leaf angles, therefore, needs more correction which is reflected in the lower DASF.

For the sun zenith as well as for the viewing angle, the findings are very similar. In line with the theory, it is predominantly the directional escape probability that is sensitive to the sun zenith (fig. 3f) and the viewing angle (fig. 4h). Both, the functions of the sun zenith angle vs. R and the viewing angle vs. R have the same form as the functions of the DASF vs. these parameters. Remembering that R is linear in the DASF, these results suggest that R is the controlling parameter. This links the gap density to the viewing angle as reported by Knyazikhin et al. (2013). For the sun zenith the dependency of R is more difficult to explain, since the directional gap density is constant for stationary viewing angle. p_1 on the other hand experiences only small variations for both parameters (fig. 3e and g) and is therefore most certainly not sensitive.

Both, the overall recollision probability, p_1, and the directional escape probability, R, show large sensitivities to biochemical constituents (fig. i-p). The sensitivity is not surprising since the within leaf recollision probability is contained in both parameters. However, the magnitude of the sensitivity is much larger than for all structural input parameters of the model.

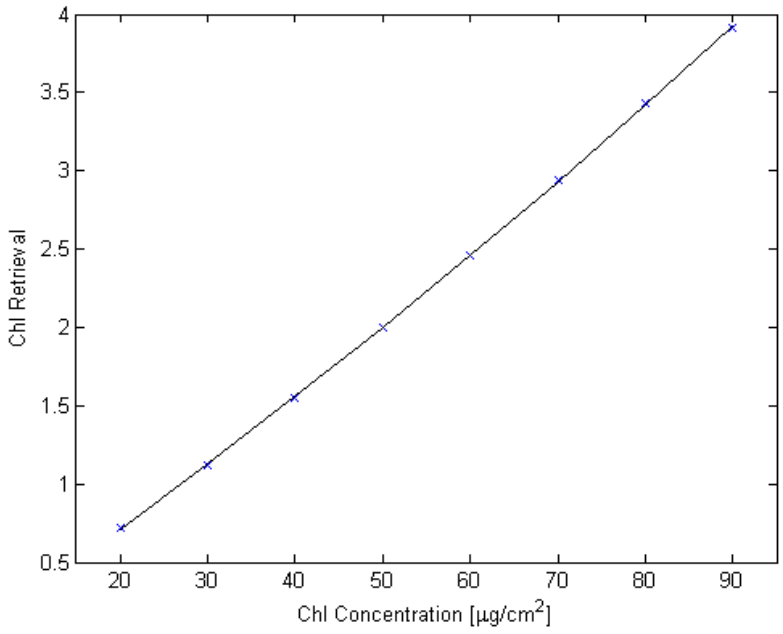

Figure 5. Relationship between PROSPECT input and retrieved chlorophyll (Gitelson et al., 2006) concentrations. $y = 0.0001x^2 * 0.0380x - 0.0736$; $R^2 = 1.00$

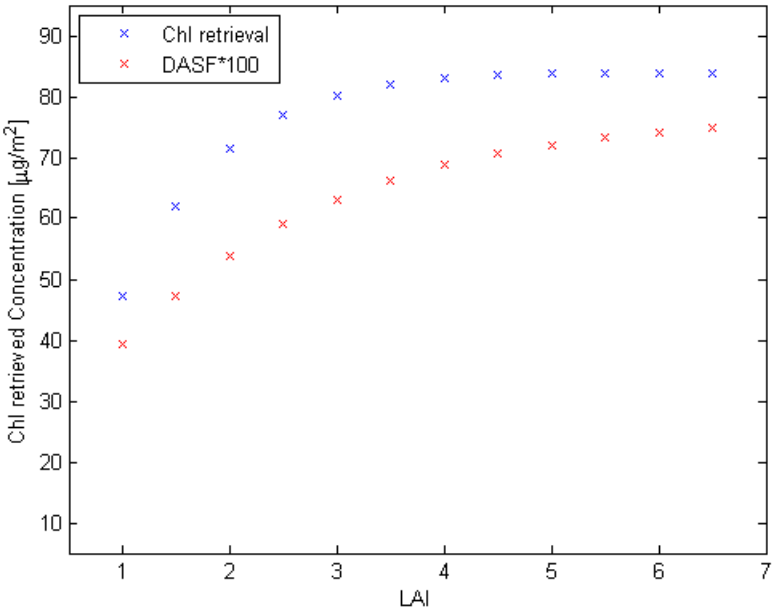

Figure 6. Retrieved chlorophyll concentration using the retrieval of Gitelson et al. (2006) combined with the relationship of figure 5 for PROSAIL simulated spectra with constant chlorophyll input concentration and varying LAi (blue). Scaled retrieved DASF from the same simulated spectra (red)

4.1.3 Pigment retrieval

The Pigment retrieval for chlorophyll of Gitelson et al., (2006) works perfectly for the simulated PROSPECT data as can be seen in figure 5. The function that relates retrieved chlorophyll content to the concentration of the input is slightly quadratic, however with a perfect correlation of 1.00. Thus, the chlorophyll retrieval of Gitelson et al., (2006) is very well suited for leaf level reflectance data.

When a canopy structure is added, however, the chlorophyll retrieval of Gitelson et al., (2006) fails to predict reliably the correct chlorophyll content. The y axis in figure 6 corresponds to the retrieved chlorophyll content of the simulated canopies transformed to real chlorophyll concentration using the function of figure 5. Figure 6 illustrates how only one structural variable, the LAI, can influence the chlorophyll retrieval through its modulation of the radiation absorption and reflectance distribution. While the input of chlorophyll concentration for all spectra of figure 6 (blue graph) is constantly 45 µg/cm^2, the retrieved chlorophyll concentrations are much higher and varying with LAI. Even for a LAI of 1 the retrieved concentration is slightly overestimated, underlining the importance of the effect of canopy structure on reflectance data. The red graph in figure 6 shows the DASF values of the corresponding canopies scaled by a factor of 100. As can be seen, the forms of both graphs are not parallel.

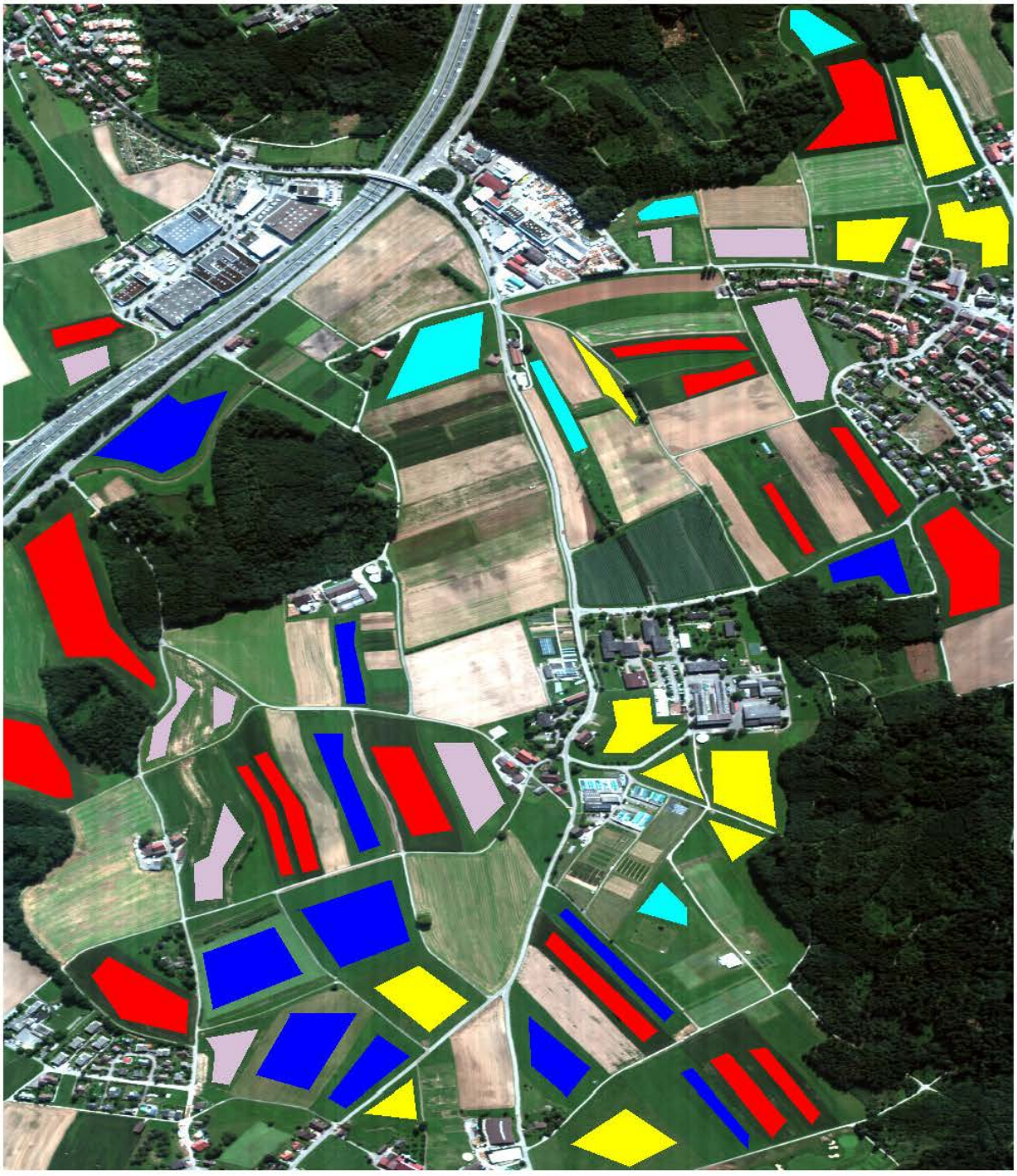

a

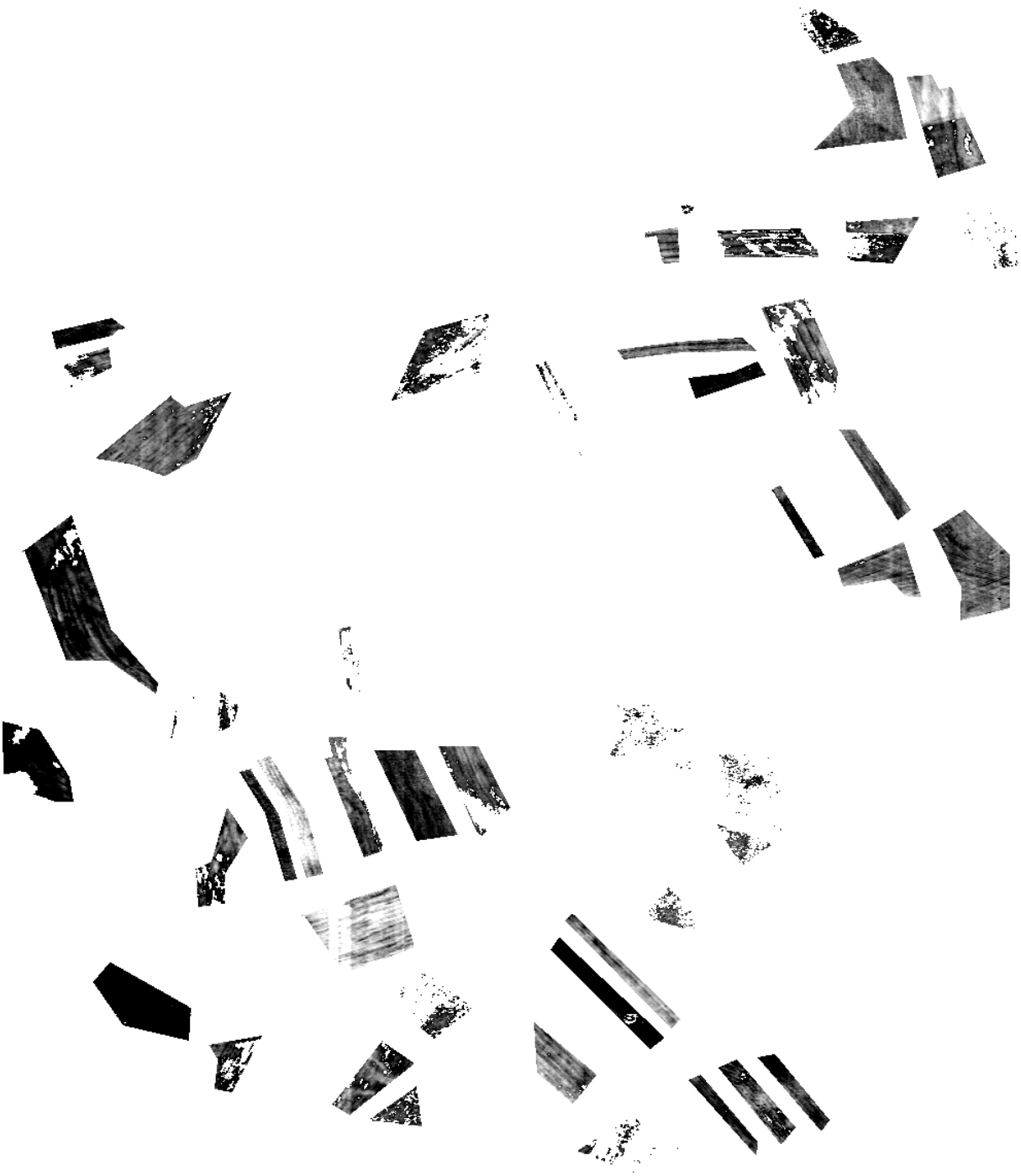

b

Figure 7. (a) True colour image of raw geometry scone of the agricultural area around Eschikon with selected fields. Red: corn, blue: temporal grassland, yellow: meadow grassland, cyan: natural grassland, thistle: sugar beet. (b) Retrieved DASF map of the selected fields after the filtering of pixels not meeting the assumptions of the retrieval (R^2).

4.2 Observational data of homogeneous canopy

Figure 7a illustrates the true colour image of the APEX scene of Eschikon in raw geometry. The regions of interest are coloured according to the crop types. Figure 7b shows the retrieved DASF map of the scene where the underlying data is already filtered from low R^2 value pixels and restricted to the regions of interest.

4.2.1 Distribution of DASF values

The pixel level distribution of DASF values from all fields is illustrated by figure 8. It has a maximum at a DASF of 0.63 with a relatively smooth distribution around it and a second small peak at 0.42. There are further a few very small values between 0.1 and 0.3. The relatively even distribution around the maximum with a second smaller peak could be indicative that only one crop type stands out in terms of a characteristic DASF. Since this smaller peak is at a very low DASF, the influence on reflectance of the canopy structure of that crop type would be high. It could therefore be corn.

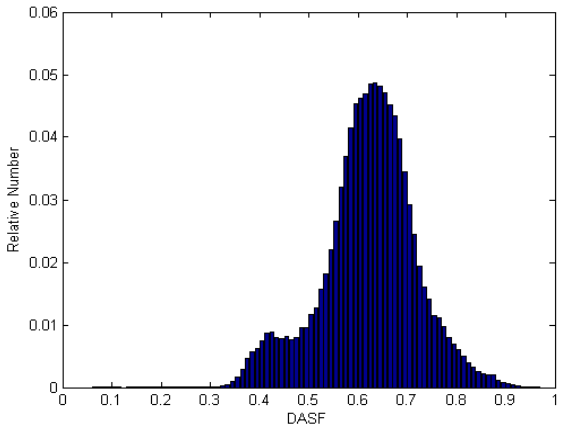

Figure 8. Distribution of DASF pixel values over all fields.

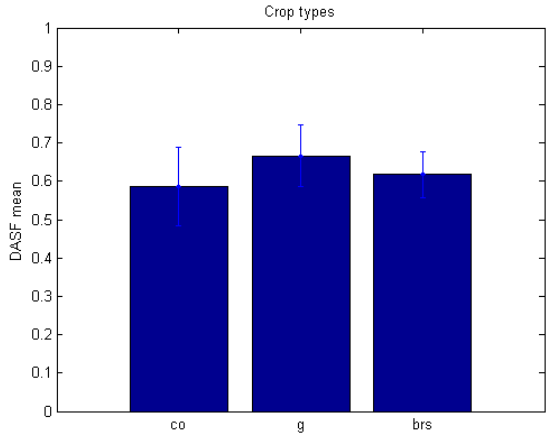
Crop types
DASF mean
co
g
brs

a

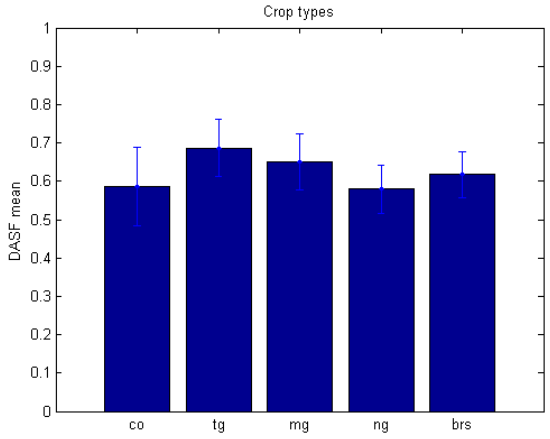
Crop types
DASF mean
co
tg
mg
ng
brs

b

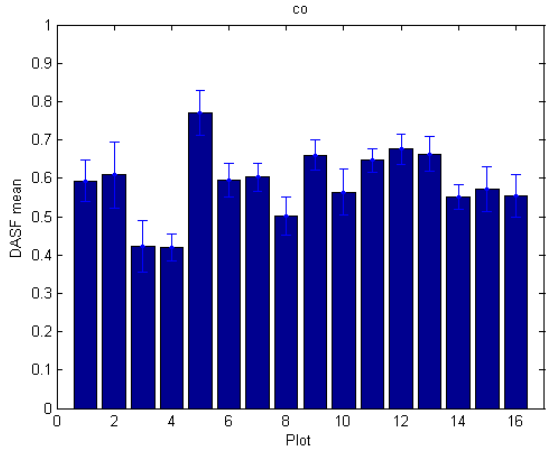
co
DASF mean
Plot

c

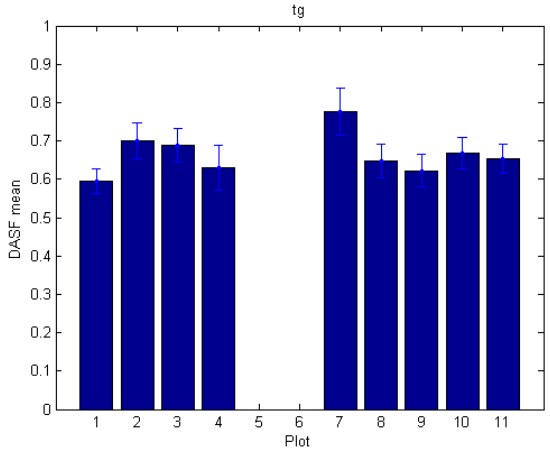
tg
DASF mean
Plot

d

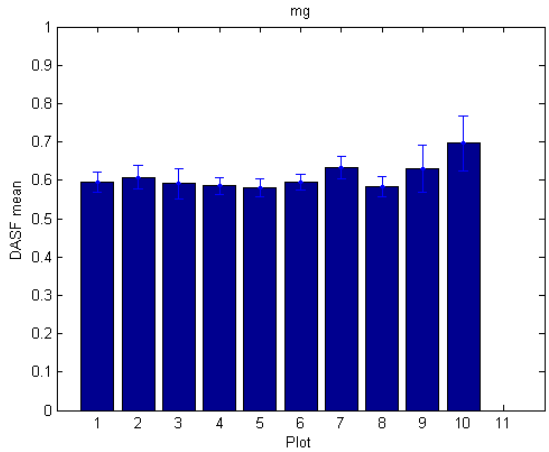
mg
DASF mean
Plot

e

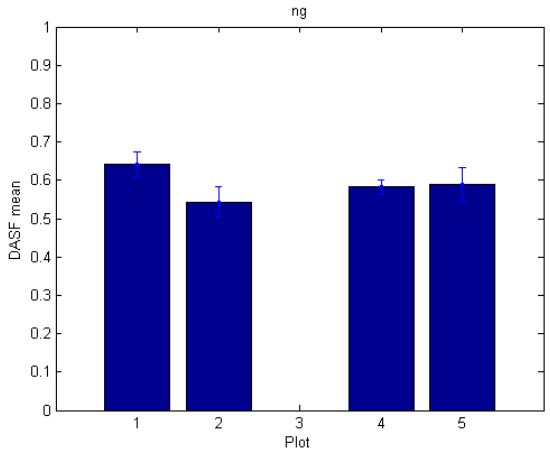
ng
DASF mean
Plot

e

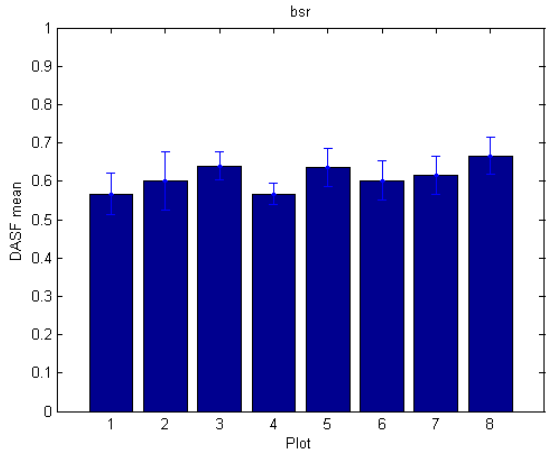

g

Figure 9. Mean DASF values and standard deviations for (a + b) each crop type, and fields of (c) corn, (d) temporal grassland, (e) meadow grassland, (f) natural grassland, (g) sugar beet. Fields without data contain no pixels that satisfy the requirements of R^2 larger than 0.998.

Figure 9a illustrates the mean DASF values and standard deviations of all the fields of one crop type taken together. The mean values (co: 0.59, g: 0.67, brs: 0.62) are spread across a small range of 0.09, suggesting that the homogeneity of the agricultural canopy is indeed reflected in the DASF values and supporting the conclusion from above that probably most crop types have similar DASF values. However, the expected crop type with a very low DASF is not found here. When separating the grass types (fig. 9b) the mean DASF values (co: 0.59, tg: 0.69, mg: 0.65, ng: 0.58, brs: 0.62) are obviously spread across a similar range of 0.11. Interestingly, a difference in the canopy structure seems to be implied for the different grass types, especially observed between tg and ng with a more influencing structure (smaller DASF) of the latter. However, this observation is weakened by the overlapping standard deviations, which suggests no clear difference between the grass types. The homogeneity between the crop types means on the other hand that these five crop types can hardly be separated according to their mean DASF values, especially considering the standard deviations. These rather large standard deviations, ranging from 0.06 to 0.10, are standing out since they are in the order of the differences between the crop types. When looking at the individual fields (fig. 9c-g) large differences in the DASF means are noticeable within one crop type with differences of at least 0.10 between fields for all crop types except bsr.

When exploring the fields that stand out from the others in the true colour and DASF scenes, some reasons might arise why they differ from the others. The fields with the lowest DASF values of co (3, 4 and 8 in fig. 9c) manifest some sparse covered surfaces within the fields where bare soil or probably a mix between vegetation and bare soil is visible, which are not masked out. This is also the case for other fields of co where such pixels show considerably lower DASF values. The small peak

around 0.42 in fig. 8 most probably comes from these pixels. This potential issue is further discussed in section 5. Field 5 of co shows larger areas of very high DASF values ranging from 0.75 to >0.8. Nothing corresponding, however, is found in the true colour image. In field 1 of tg darker stripes with low DASF values are visible probably originating from a tractor. Field 7 of tg demonstrates similar areas of high DASF as field 5 of co, with values even ranging from 0.8 to 0.95. But again no evidence for a cause of such high DASF values is found in the true colour image. By looking very carefully at field 11 of mg one can distinguish two separate grass fields in the RGB image. These two fields are much more pronounced in the DASF scene, which is probably the reason for the outlying DASF mean and the larger standard deviation.

By taking these issues into consideration, the distribution of the DASF values gets a little bit more homogenous for the examined agricultural canopy, especially the high variation between fields of one crop type. Despite the better picture, variations within fields remain higher than expected and therefore suggesting a rather heterogeneous canopy.

Further investigations of the fields show that in most co fields stripes barely visible on the true colour scene are, however, very prominent on the DASF map. Because these stripes are always oriented longitudinal to the field boarders, they are presumably stemming from tractor tracks. These tracks are probably the main contributors to the variation in the DASF within the fields of co as they show lower values (e.g. 0.52-0.65 for the tracks compared with 0.63-0.72 between the tracks for field 13). This could either mean that the tracks would add some kind of structure to the otherwise more homogeneous canopy of co, or that the DASF retrieval, like for the bare soil surfaces, does not work properly for the tracks. Since the tracks are green in the true colour image, it is assumed that the vegetation is dense enough and that the lower DASF values therefore come from the added structure of the tracks. Such longitudinal stripes are also present in other fields, especially the ones of brs. In addition, even though brs should be very dense and ground covering at this stage of growth, the true colour image reveals sparse covered areas with sometimes even visible bare soil. These areas are often masked out, but the same problem as for co emerges. Although the masking works better for brs, there are still unmasked pixels that should be filtered. Similarly, grassland fields, mainly mg and ng, show even larger areas scattered across the fields masked out by the R^2 filter. It is not clear whether this comes from the young age, the sparser crop type or another reason not evident here, but it is an indication that the spectral invariant theory may not work properly for these types. The areas of very high DASF values present in some fields on the other side could indicate a high LAI, as section 4.1.1 would suggest.

The overall picture of a homogeneous agricultural canopy is in the end not reflected in the DASF. Apparently, different effects are present on this spatial level.

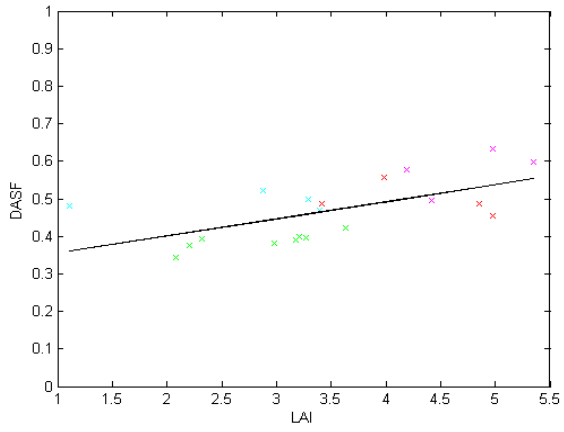

a

R^2 = 0.383, n = 20

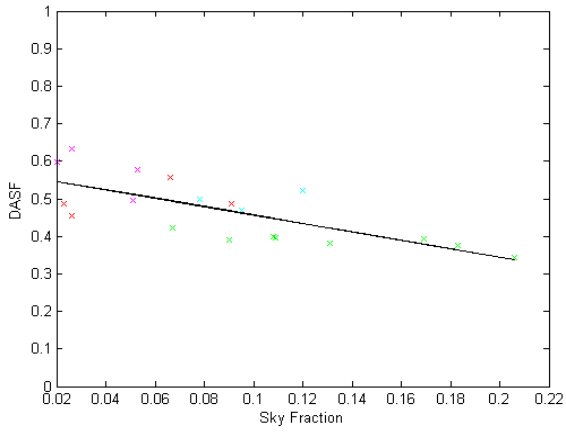

b

R^2 = 0.542, n = 20

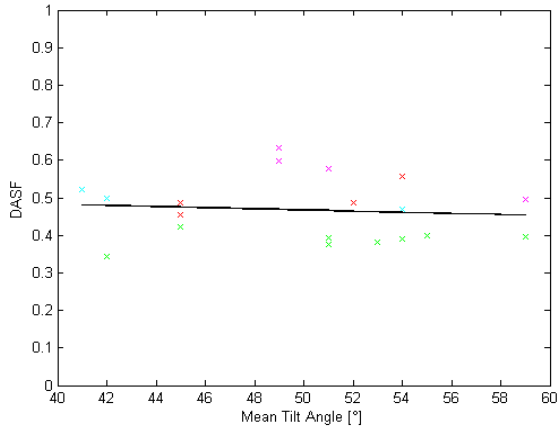

c

R^2 = 0.010, n = 20

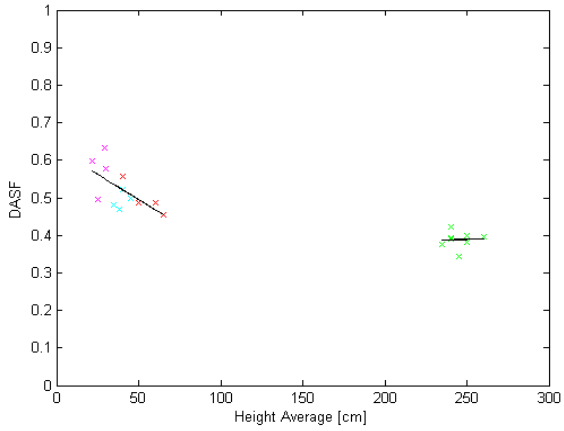

d

R_1^2 = 0.406, n = 12 ; R_2^2 = 0.002, n = 8

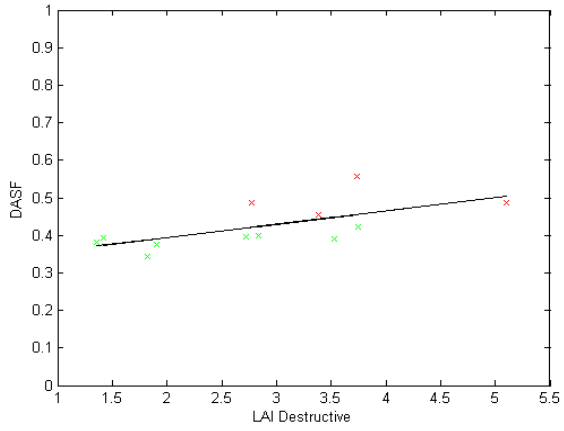

e

R^2 = 0.423, n = 12

Figure 10. Sensitivity analysis of DASF to (a) LAI, (b) Sky fraction, (c) Mean tilt angle, (d) Canopy height, (e) LAI destructive. Green: corn; red: soybean; cyan: sugar beet; magenta: temporal grassland. Plots without pixels satisfying the requirements of R^2 larger than 0.98 are not shown.

4.2.2 Sensitivity of DASF to in situ retrieved structural parameters

The figures 10a-e illustrate the sensitivity of the DASF to in situ retrieved structural parameters of the 2x2m plots. It is stated here that one needs to be very careful with these results and the ones of the following section, since the number of data points used is rather low. This makes the correlation prone to outliers. Also, there are different crop types involved that may need a separate consideration. However, for a first investigation this data provides valuable insights for the behaviour of the DASF and its relation to more concrete parameters.

As expected, the DASF correlates with the LAI and LAI destructive with a R^2 of 0.383 and 0.423 respectively (fig. 10a and e). These findings support the probable link between the recollision probability and the LAI already mentioned in the results of section 4.1.1. This relationship could be a reason for the areas of very high DASF values found in section 4.2.1 for co and tg, suggesting high LAIs for these areas. For higher LAIs, the DASF should experience a saturation effect as shown by section 4.1.1. This effect is not visible here, eventually due to the few data points.

Three effects that influence the DASF in different directions are linked to the sky fraction. The most straight forward effect is that a lower sky fraction directly means that the canopy interceptance is higher and therefore also the DASF. A lower sky fraction also results in a lower escape probability and therefore a higher recollision probability. This effect makes the DASF higher as well. On the other side, a lower escape probability also results in a lower directional escape probability for flat canopies (Knyazikhin et al., 2013). This effect lowers the DASF in contrast. The comparatively high R^2 of 0.542 for the negative correlation with the sky fraction (fig. 10b) suggests that either the effects of the canopy interceptance and/or the recollision probability predominate. The next section will further break this relationship down to provide more insight.

The mean tilt angle of the leaves is nearly not correlated with the DASF (R^2 = 0.010), therefore suggesting no relationship between these two parameters (fig. 10c). This missing relationship is not in line with the theory and the explained findings of the simulation section 4.1.1. The lack of relationship probably originates from unreliable in situ measurements for the mean tilt angles of the plots.

The DASF shows a comparably good sensitivity (R^2 = 0.406) to the height average of the plots of sb, brs and tg, while no correlation is evident for co (fig. 10d). The first result is consistent with a set of studies between height measurements and spectral invariants (Heiskanen, 2006; Kimes et al., 2006; Schull et al., 2007). Schull et al. (2007a) and Wang et al. (2011) for example find correlations between canopy heights retrieved from the escape probability and such from LiDAR measurements. However,

this relationship seems missing for co. On the other hand, interpolating both functions could suggest that the DASF curve is flattening with height for crop canopies. This interpretation of the data is very hypothetical since no data points are available in between. The negative correlation for sb, brs and tg would mean that for higher vegetation, more radiation is absorbed as a result of the canopy structure. This indicates either a higher recollision probability, lower directional gap density, lower canopy interceptance or a mix between these. Again, the next section will hopefully give more insight about this relationship.

4.2.3 Sensitivity of overall recollision and directional escape probabilities to in situ retrieved structural parameters

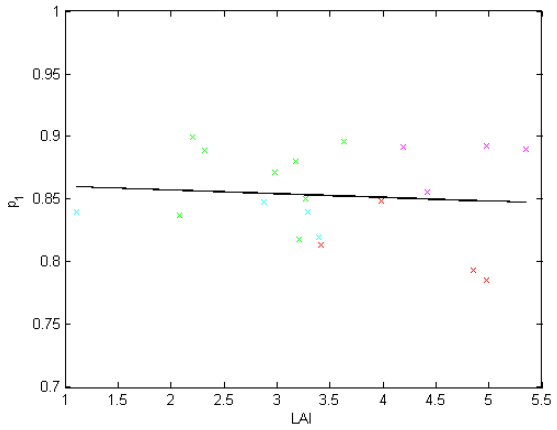

a

$R^2 = 0.008$

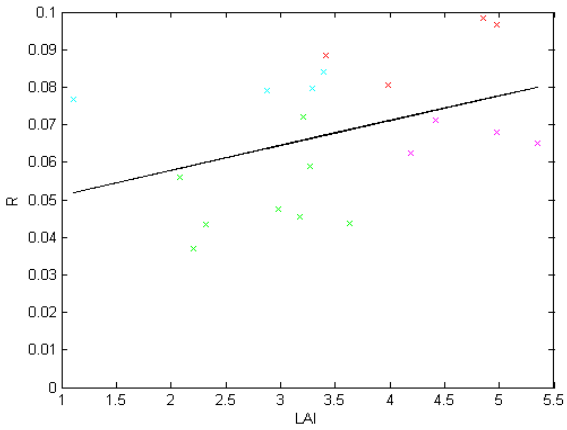

b

$R^2 = 0.159$

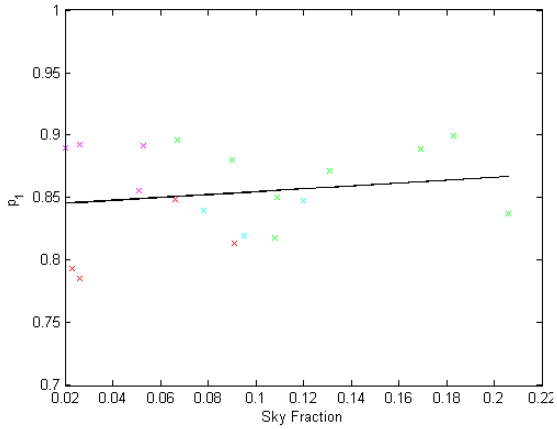

c

$R^2 = 0.029$

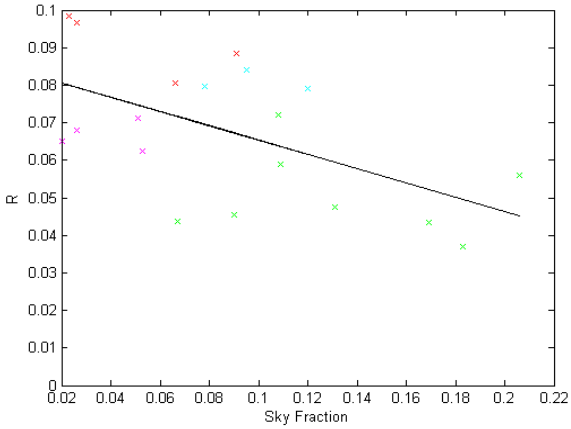

d

$R^2 = 0.314$

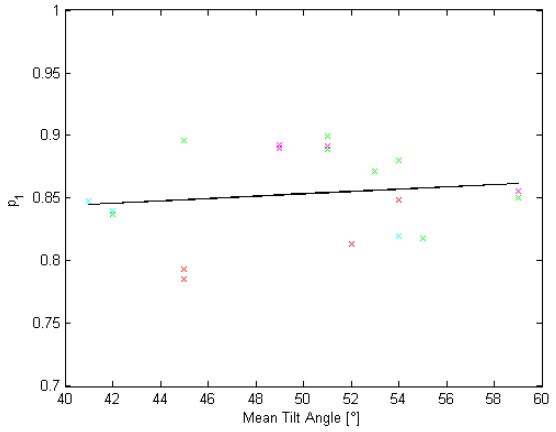

e

$R^2 = 0.020$

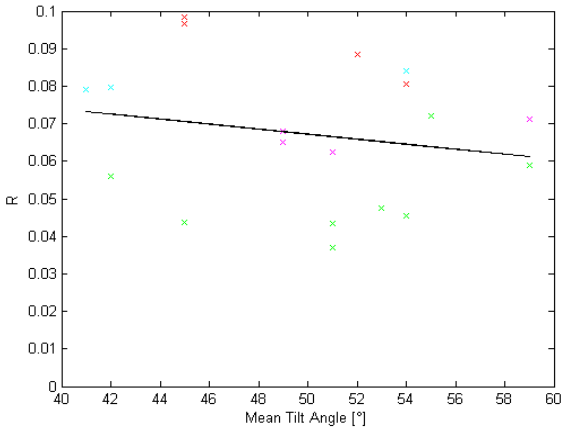

f

$R^2 = 0.038$

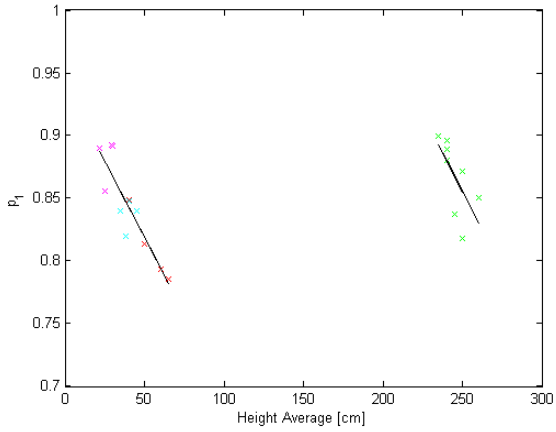

g

$R_1^2 = 0.799$; $R_2^2 = 0.457$

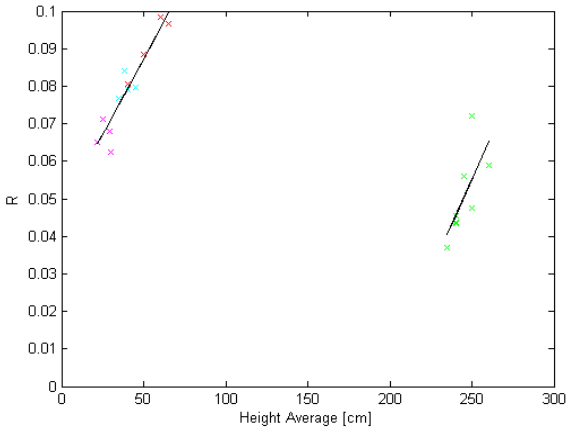

h

$R_1^2 = 0.882$; $R_2^2 = 0.510$

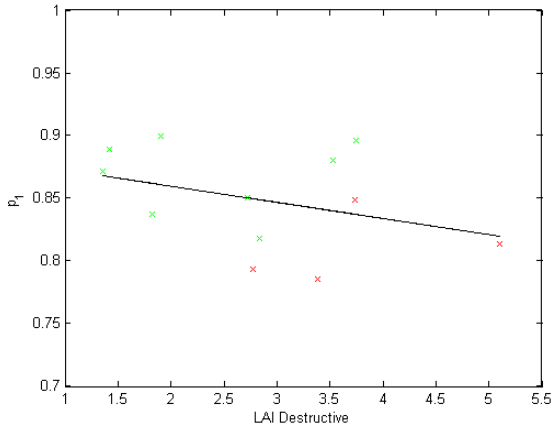

i

$R^2 = 0.126$

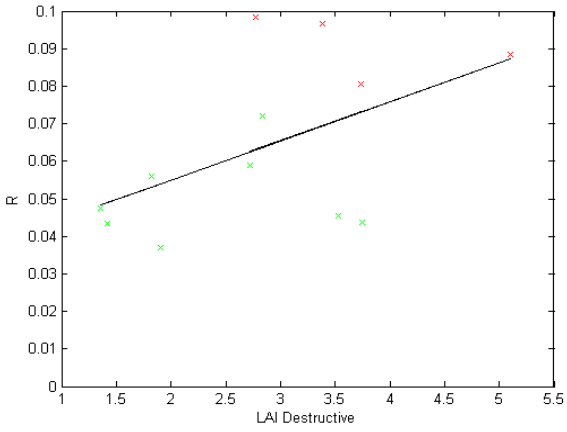

j

$R^2 = 0.271$

Figure 11. Sensitivity analysis of p_1 and R to (a + b) LAI, (c + d) Sky fraction, (e + f) Mean tilt angle, (g + h) Canopy height, (i + j) LAI destructive. Green: corn; red: soybean; cyan: sugar beet; magenta: temporal grassland. Plots without pixels satisfying the requirements of R^2 larger than 0.98 are not shown.

To further decouple the effects of the structural parameters on the DASF, the directional escape probability, R, and the overall recollision probability, p_1, are considered separately (fig. 11a-j). It is noticeable that the quality of the sensitivities is generally very low, except for the ones to the canopy height.

Despite the expected correlation between the DASF and the LAI in the previous section, the correlation analysis between the overall recollision probability and the two LAIs (fig. 11a and i) and the directional escape probability and the two LAIs (fig. 11b and j) show rather bad results. While the overall recollision probability is comparably not/weakly correlated with the two LAIs (R^2 of 0.008 and 0.126), the directional escape probability is weakly/moderately correlated with both LAIs (R^2 of 0.159 and 0.271). Especially the missing correlation between p_1 and the LAI is not comparable with previous studies comparing p to LAI (Mõttus, 2007; Rautiainen et al., 2009) and the PROSAIL section.

As mentioned in 4.2.2, a varying sky fraction can impact the DASF through different effects. The figures 11c and d entangle these effects nicely. While p_1 shows no correlation, R is moderately correlated negatively with the sky fraction. Therefore, the sensitivity of the DASF to the sky fraction arises probably from the sensitivity of the canopy interceptance. This result also presents the most straight forward explanation of the relationship between sky fraction and DASF (4.2.2).

The mean tilt angle is neither correlated with p_1 nor with R (fig. 11e and f), but as supposed in section 4.2.2 it is most certainly due to the non-reliable in situ measurements of the mean tilt angle of the plots.

A surprising result is displayed by the figures 11g and h. While the expected and reported strong relationship between recollision probability and canopy height is also presented here for p_1 (R^2 = 0.799 and 0.457), R shows an even higher correlation with the canopy height. However, both correlations are in opposite direction than one would expect, since p_1 is negatively and R positively correlated with canopy height. Interpreting these results would mean that the larger the vegetation volume is the lower the overall recollision and the higher the escape probability. This is in fact opposite to the theory. Furthermore, the opposite correlations for p_1 and R lead to a cancelling effect for co in the sensitivity of the DASF to crop height, whereas the sensitivity of p_1 seems to dominate for the other crop types.

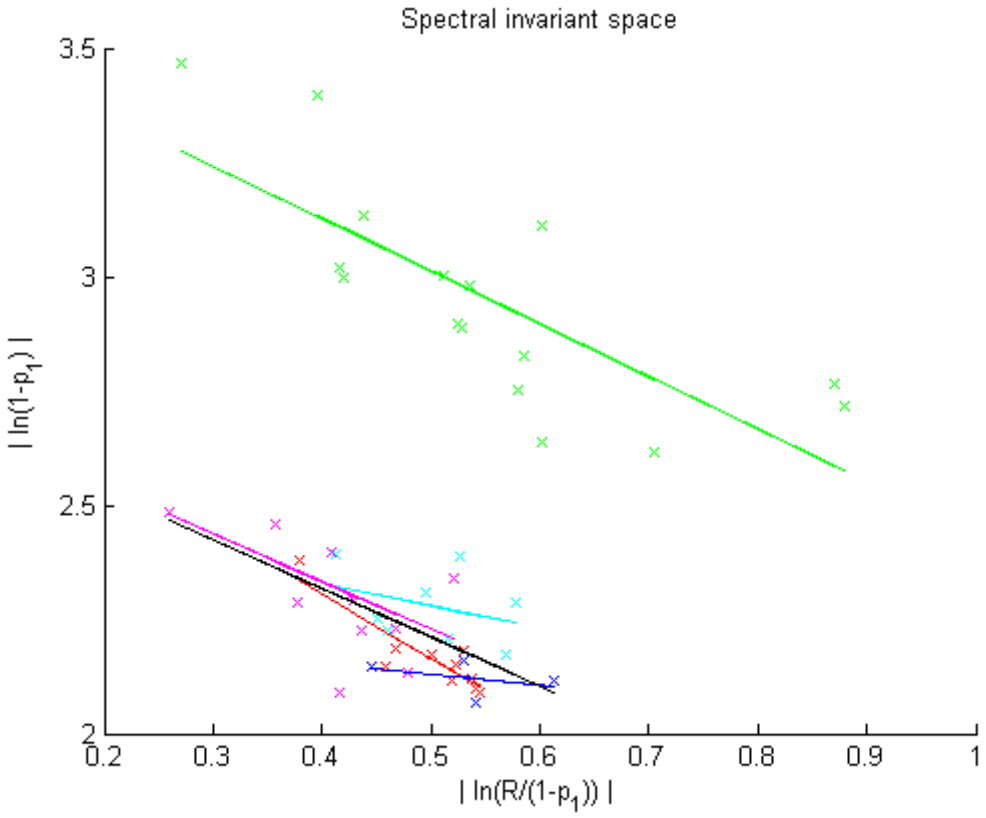

Figure 12. Spectral invariant space for field level data. Green: corn (R_2 = 0.59), cyan: sugar beet (R_2 = 0.13), red: meadow grassland (R_2 = 0.78), blue: natural grassland (R_2 = 0.15), magenta: temporal grassland (R_2 = 0.49), black: sugar beet, meadow, natural, temporal grassland (R_2 = 0.48). Fields without pixels satisfying the requirements of R^2 larger than 0.998 are not shown.

4.2.4 Crop discrimination in the spectral invariant space

While the crop types were not separable with the DASF, corn obviously separates itself from the other crop types in the spectral invariant space (Fig. 12). As expected, all crop types are scattered across a similar range of the macro structure values (x-axis), strengthening the evidences found in 4.1.1 that the crop types have DASF values in a comparable range. The y-axis, however, shows that corn has a clearly different micro structure than the other crop types, meaning that the leaf density and/or distribution of corn are distinguishable from the others. This makes certainly sense when thinking of a corn canopy. The leaf distribution is different for corn due to the leaf form and orientation and the crop height than for the low but dense grass types and the sugar beet with its rather low canopy and horizontal leaves. This difference is enough to separate corn from the other crop types in the spectral invariant space. Despite lying on different lines in the space, the other crop types cannot be separated from each other since they are all located in the same area. Very similar results are obtained by Carmona et al. (2010), where corn is also separable from the other crop types.

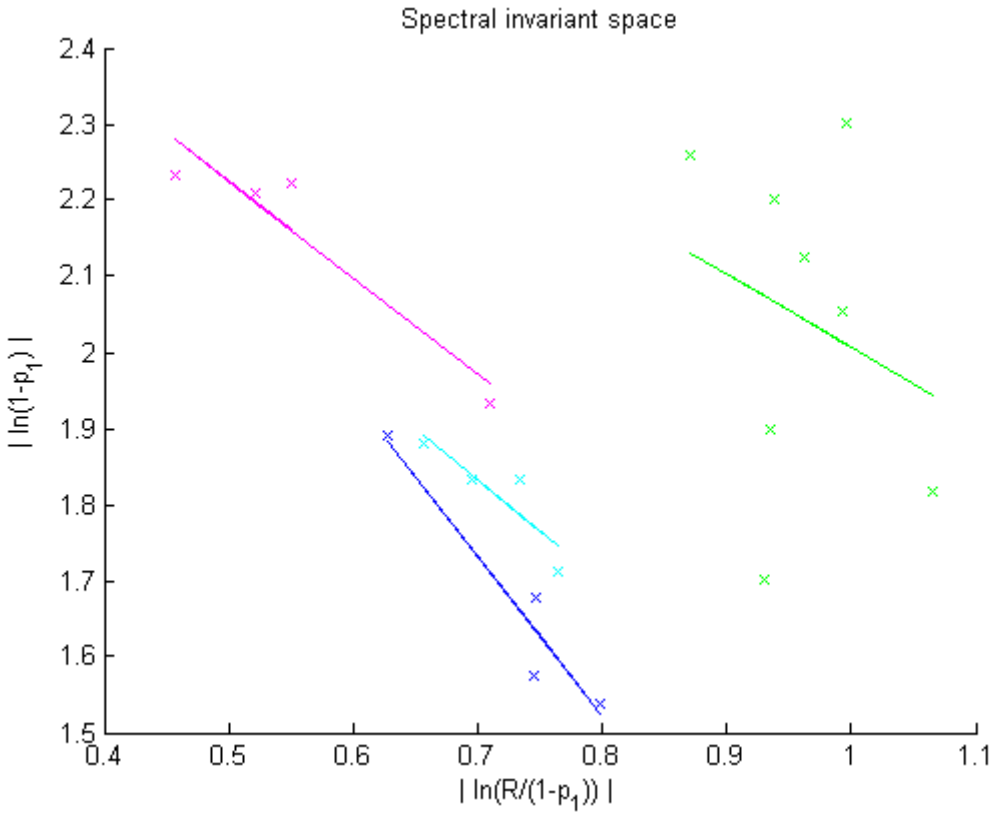

Figure 13. Spectral invariant space for plot level data. Green: corn (R^2 = 0.07), cyan: sugar beet (R^2 = 0.78), magenta: temporal grassland (R^2 = 0.89), blue: soybean (R^2 = 0.92). Plots without pixels satisfying the requirements of R^2 larger than 0.98 are not shown.

When applying the spectral invariant space to the data from the plots used for the sensitivity analysis of spectrally retrieved to in situ retrieved structural parameters, a different result is obtained (fig. 13). The crop types of sugar beet, temporal grassland and soybean still lay on a comparable line as before, however, with temporal grassland being separable from sugar beet and soybean especially due to the lower values of the micro structure of sugar beet and soybean. The biggest difference compared with figure 12 is corn which is placed in a totally different place with no visible relationship between the macro and micro structure. It is still separable from the other crop types, but this time due to the macro structure. The range of the micro structure values, which was the main difference between corn and the other crop types when looking at the mean values of the fields, is the same as for the other crop types. The reason why corn is separable from the other crop types in this analysis is, therefore, totally opposite to the one before.

4.3 Observational data of heterogeneous canopy

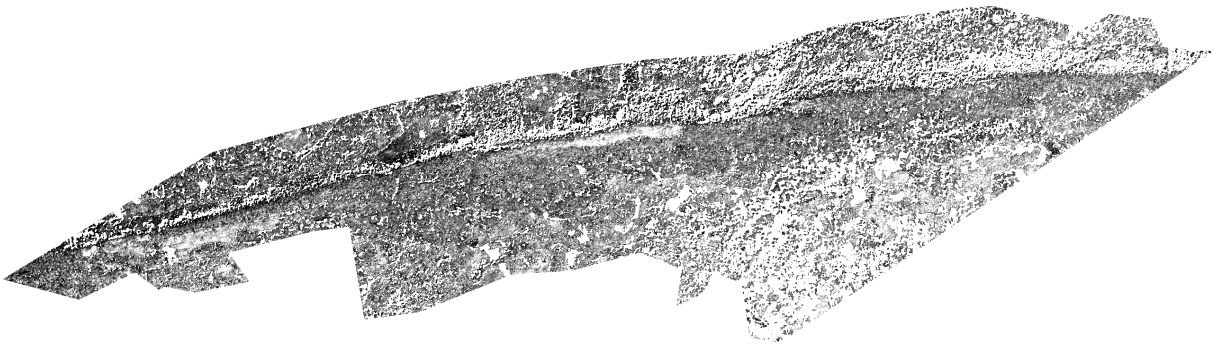

Figure 14. DASF map of the Lägern forest area with applied R^2 and shadow filter (white pixels). Dark pixels represent low DASF values.

4.3.1 Distribution of DASF values

The figures 15a and b show the distribution of the DASF pixel values for the Lägern forest scene (fig. 14) in the original 2m and resampled 8m resolution respectively. The distribution of the 2x2m resolution is smoothly distributed around the most frequent value of 0.52 with a median of 0.58. The distribution of the 8x8m resolution is flatter on top with the most frequent value of 0.535 which is also the median. Since especially the distribution of the 2m resolution scene is unimodal, no canopy structure type seems distinctive yet and the distribution could suggest evenly distributed DASF values for all canopy structure types. This, however, seems much more unlikely than for the homogeneous canopy because the differences in the macro structure between the different canopy structure types should definitely be more pronounced.

Figure 15c illustrates the difference of the two distributions subtracting the distribution of the 8m from the 2m resolution. It emphasises how the distribution of the 8m resolution is more shifted towards lower DASF values compared with the 2m resolution.

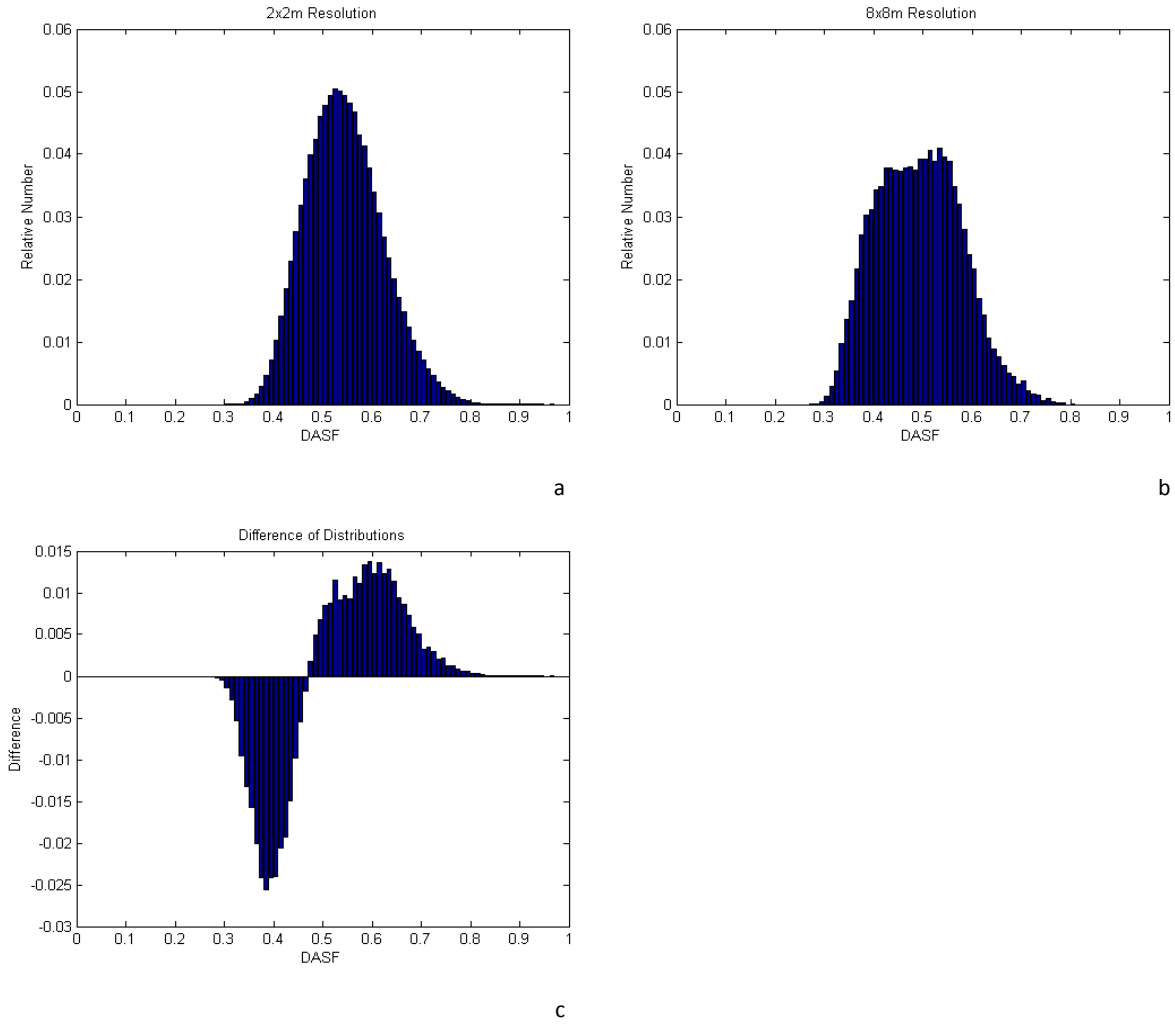

Figure 15. Distribution of DASF pixel values of the Lägern forest area at (a) 2m resolution, (b) 8m resolution. (c) Difference of (a) and (b).

Compared with the homogeneous canopy (fig. 8) the heterogeneous canopy (fig. 15a) shows smaller DASF values. This suggests, as expected, a larger influence on reflectance from the higher and more complex forest canopy as opposed to the agricultural canopy. When looking at the different exposed areas, however, a difference in the distribution of DASF values is clearly visible. The norther hillside, which is less exposed to the sun, shows smaller DASF values (fig. 16a) than the southern hillside (fig 16b). When comparing the south side of the Lägern forest with the agricultural canopy, first still show smaller DASF values than latter. Therefore, the suggested higher influence of the forest canopy structure is probably valid.

Comparing the DASF values of the canopy structure types, no CST (fig. 1) is distinctive when looking at the mean DASF values and standard deviations as suggested by figure 17. The differences between the mean values are even smaller than the ones of the crop types ranging from 0.44 to 0.52 but with comparable standard deviations ranging from 0.07 to 0.1.

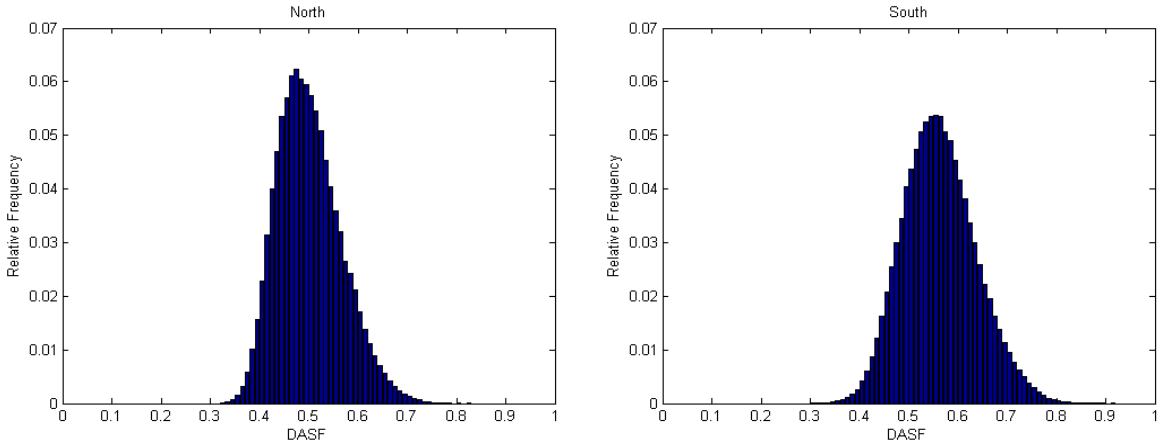

a b

Figure 16. Distribution of DASF pixel values of (a) the northern hillside, (b) the southern hillside the Lägern forest area.

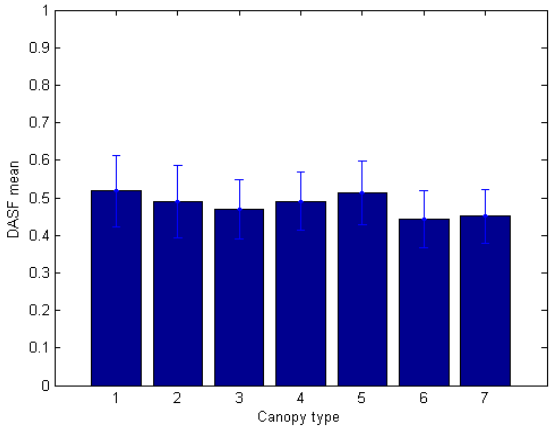

Figure 17. Mean DASF values and standard deviations for each of the canopy structure types.

4.3.2 Sensitivity of DASF to LiDAR-derived structural parameters

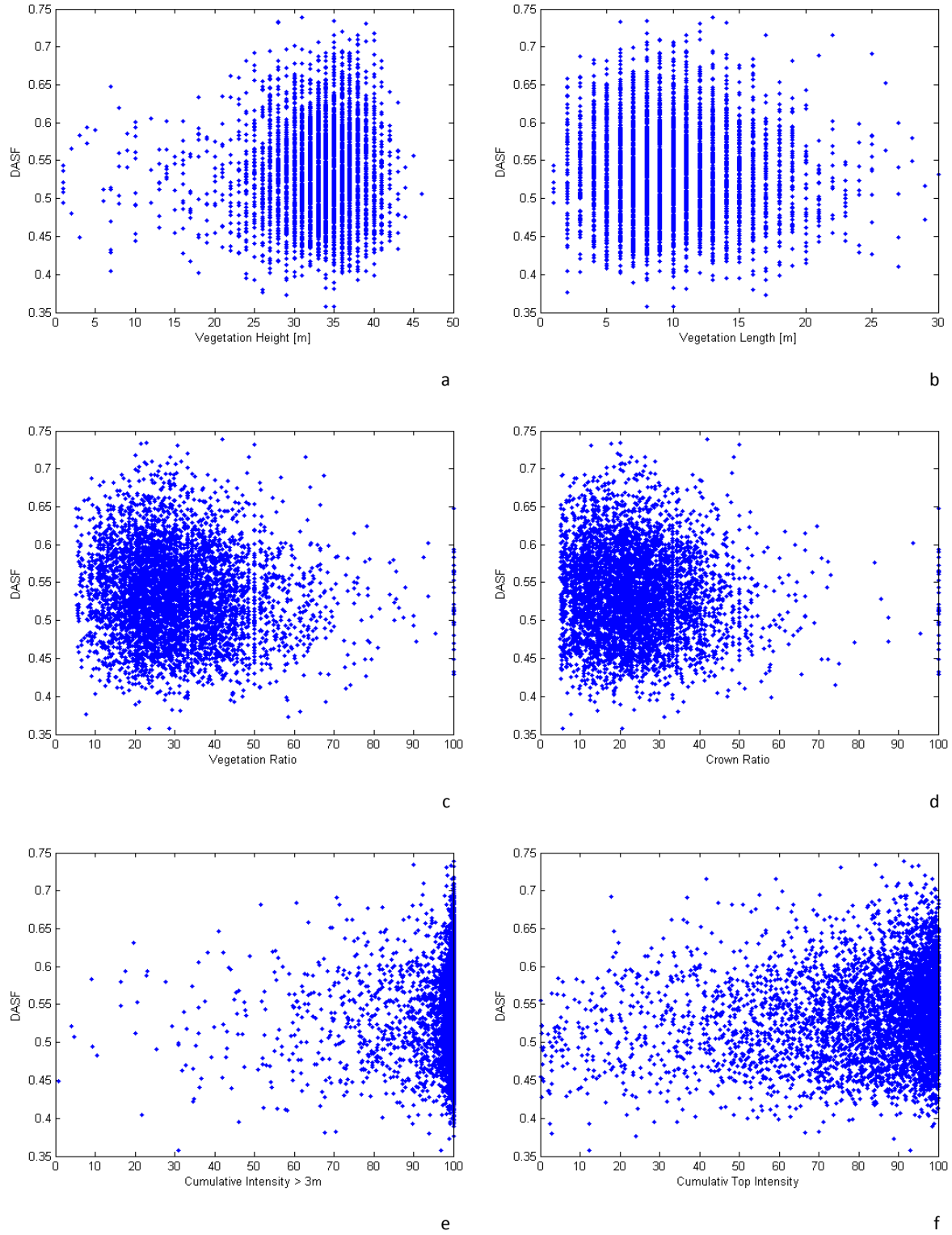

Figure 18. Sensitivity analysis of DASF to (a) Vegetation height, (b) Vegetation length, (c) Vegetation ratio, (d) Crown ratio, (e) Cumulative intensity above 3m from ground, (f) Cumulative top intensity.

The results from the correlation analysis between the DASF and the first set of LiDAR retrieved structural parameters are illustrated by the figures 18a-f. No sensitivity of the DASF to neither of the parameters is found, which is very surprising. The relationship between canopy height and spectral invariants has been shown by different studies (Heiskanen, 2006; Kimes et al., 2006; Schull et al., 2007) and was also found in the sections 4.2.2 and 4.2.3. However, no trend or pattern is indicated here (fig. 18a). The DASF was also expected to be related to the cumulative intensity of the top three meters of the canopy (fig. 18f) since a higher intensity is indicative for a more closed canopy crown. This should result in a higher DASF because less radiation would enter the canopy, interact with it and get absorbed or scattered away. Instead, the DASF values look rather randomly distributed over the parameter range in the plots of the figures 18. One conclusion could be that the DASF is not related to these parameters. This, however, seems very unlikely for the reasons mentioned above.

The figures 19a and b show the sensitivity of the DASF to the difference between the height of the first 1% of points and the height of the first 10%, respectively 20%, of points registered by the LiDAR sensor as echo. The figures 19c and d show the same, but for the relative density of the first two bins from top of the canopy. For these two analyses one would expect a similar result to the one expected for figure 18f. If less echo points are registered on top of the canopy over a longer distance (fig. 19a and b), the canopy is expected to be less dense. Therefore, more radiation would be able to penetrate into the canopy and interact with it. The same is valid for the density of the first, or respectively second, two meters (bin 1 or 2) from top of the canopy (fig. 19 c and d). Unfortunately, neither sensitivity nor other pattern is found here. This is less surprising, since these two parameters stem from the same dataset as the ones of figures 18a-f.

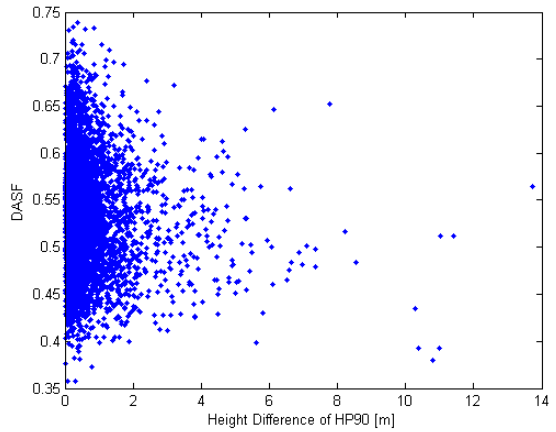

a

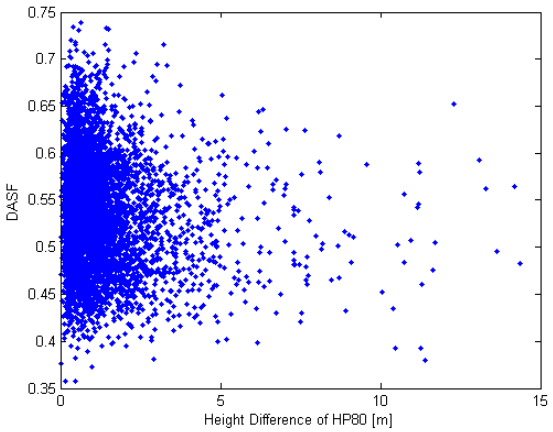

b

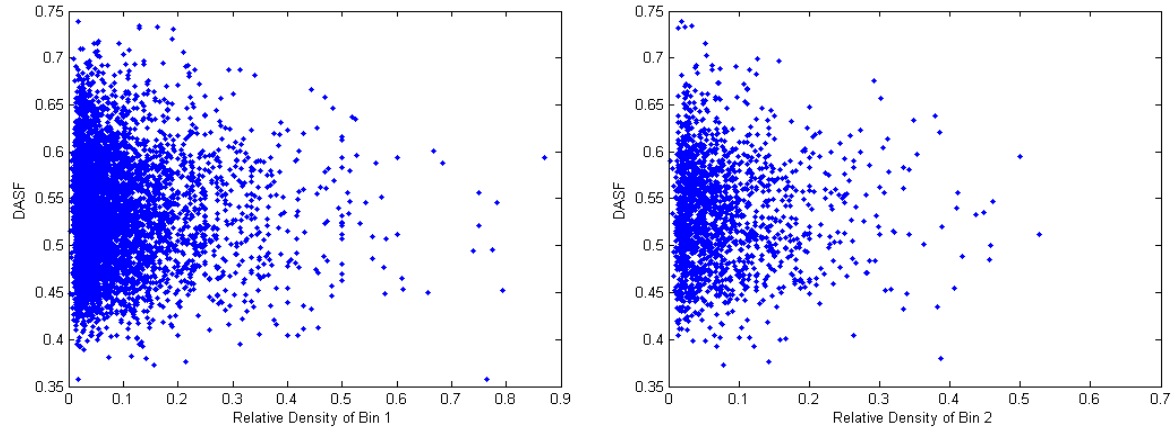

Figure 19. Sensitivity analysis of DASF to (a) difference of vegetation height to height where 90% of points lay beneath, (b) difference of vegetation height to height where 80% of points lay beneath, (c) Relative density of top bin, (d) Relative density of bin 2.

The last analysis for the heterogeneous canopy compares the DASF to the second set of a LiDAR derived structural parameter, the PAI (fig. 20a to d). Again, a smaller PAI on top is indicative for a less dense canopy there. Hence, more radiation is able to enter the canopy, interact with it and get absorbed or scattered away. However, as for the other analysis of this section, no sensitivity is found for the DASF to relative PAI of the top 4 meters of the canopy (fig. 20 a and b). The figures 20c and d show that the DASF is similarly distributed for all PAI intervals. The interpretation of this would mean that the density of the canopy top layer does not affect the DASF, which is a parameter incorporating different structural parameters. However, it is shown at the beginning of this chapter (fig. 3a and 10a) and in the sections 4.1.1 and 4.2.2 that the LAI, for example, influences the reflectance and therefore the DASF as explained above. Therefore a correlation between the DASF and the PAI values of the top layers would be highly conceivable.

The same analysis was also performed for the different CSTs. However, they are not presented here since they do not show any relationship as well.

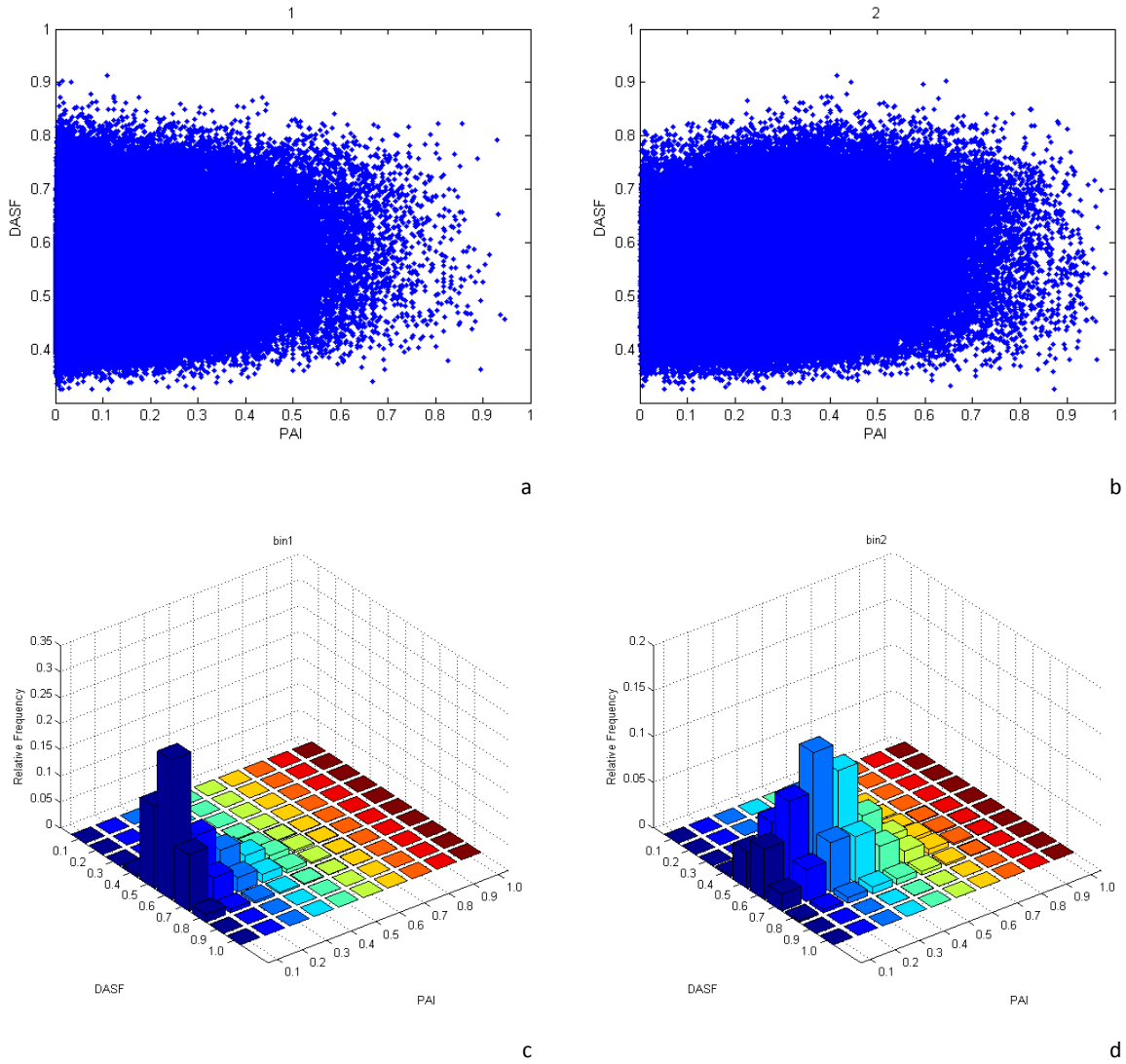

Figure 20. Sensitivity analysis of DASF to PAI of (a) top bin, (b) second bin. Relative frequency distribution of the pixels between DASF and PAI values of (c) top bin, (d) second bin.

4.3.3 Canopy type discrimination in the spectral invariant space

Contrary to the homogeneous canopy where at least some differences between crop types are visible in the spectral invariant space for averaged field values (fig. 12) and on plot-level (fig. 13), no discrimination of canopy types is found for the Lägern forest (fig. 21). Although the points lie more or less on a line, the different canopy types are not grouped in characteristic areas in the space as for example in Knyazikhin et al. (2009) and Schull et al. (2011).

One reason could be the use of the pixel-level data of p_1 and R. Some results from sections of the homogeneous canopy already suggest that the retrieval of p_1 and R, and therefore also the DASF, is not always reliable on a smaller pixel size.

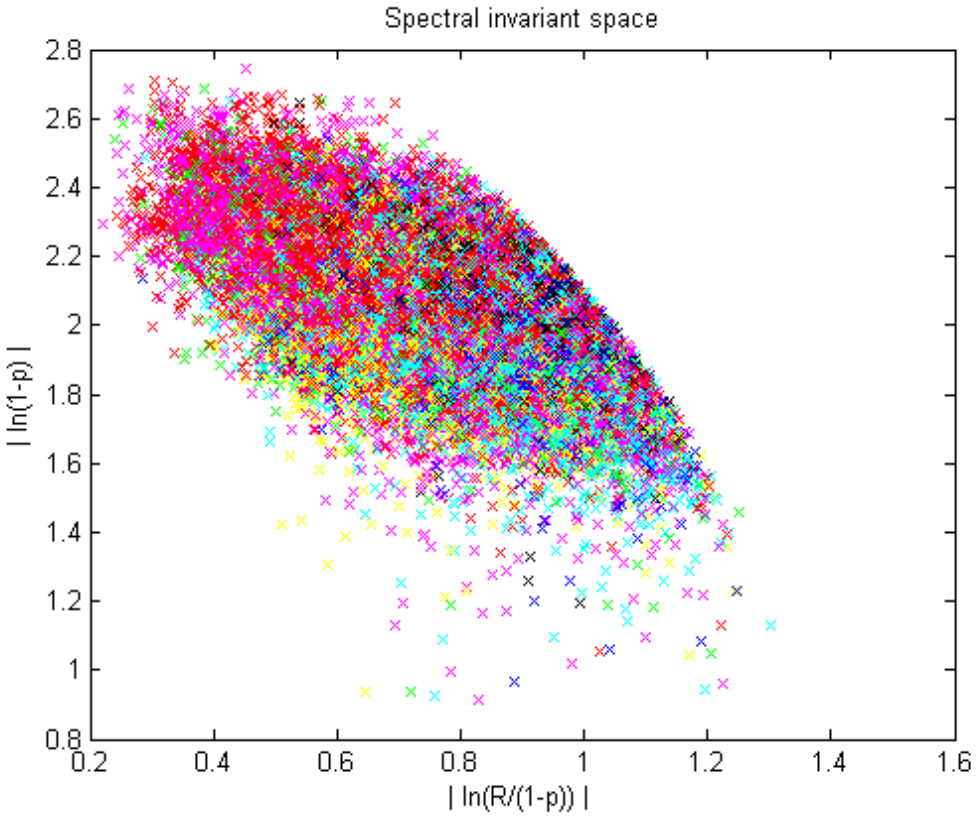

Figure 21. Spectral invariant space for the Lägern forest area. Green: CST1, magenta: CST2, cyan: CST3, yellow: CST4, red: CST5, blue: CST6, black: CST7.

4.4 Leaf biochemical constituent retrieval

4.4.1 Three-band Method with canopy structure

As expected and already experienced in section 4.1.3, the chlorophyll retrieval of Gitelson et al. (2006) is struggling as soon as a canopy structure is present. This is further shown by figure 22, where no relationship between the in situ retrieved chlorophyll content and retrieved chlorophyll content using the method of Gitelson et al. (2006) is found.

4.4.2 Leaf biochemical retrieval method derived from spectral invariants theory

The different specific absorption spectra for the biochemical constituents used in the LUT are shown in figure 23a. While the structure parameter has a constant but slow specific absorption over the whole spectrum, the other constituents possess characteristic absorption peaks.

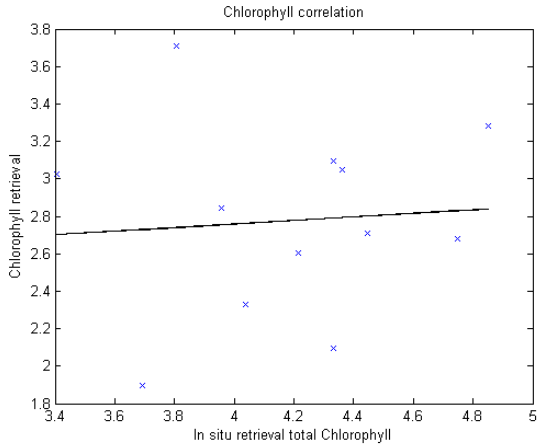

Figure 22. Comparison of in situ retrieved total and retrieved (Gitelson et al., 2006) chlorophyll content.

Figure 23b illustrates an example taken from the analysis of the biochemical constituent retrieval. It represents the absorption spectra of a pixel of corn field number 1. The blue curve shows the absorption retrieved using the mean DASF and p_1 of the field and applied on the spectrum of the pixel (right hand side of the equation). The red curve represents the lowest absorption spectrum of the LUT (structure parameter: 1.6; chlorophyll: 30 µg/m^2; carotenoids: 2 µg/m^2; equivalent water thickness: 0.015 cm; dry matter: 0.008 g/cm^2). This leaf biochemical composition is assigned by the algorithm to nearly all pixels of the field. There is a large discrepancy in y-direction between the retrieved absorption spectra and the ones from the LUT. Since all other absorption spectra from the LUT are positioned even higher than the one shown here, the RMSE between retrieved spectra and LUT spectra is always smallest for the spectrum with the smallest constituent concentrations. When further comparing the two curves both show a similar progress throughout the wavelengths, but there is a shift between the two spectra and the local maxima are much more pronounced in the simulated spectrum relative to the retrieved spectrum. By shifting the blue curve by 1 and multiplying it afterwards by 3, both in the y-direction, the two curves become comparable (cyan curve). When analysing the two curves now, it is apparent that except the local maximum around 675nm every other local maximum or minimum is shifted between the retrieved and simulated absorption spectrum. Moreover, the shifts are not constant. While the maximum around 1480nm of the retrieved spectrum is shifted towards higher wavelengths by 40nm compared to the simulated spectrum, the maximum around 1910nm of the retrieved spectrum is shifted towards smaller wavelengths by 20nm. Figure 14b also illustrates that the retrieved spectrum has more local maxima (630nm, 1205nm, 1880nm, 2115nm, 2060nm and a few around 2320nm) than the simulated spectrum. However, this is probably because the water parameter is set so high that its absorption overwhelms the one of dry matter where the peaks of 1205nm and higher probably originate from.

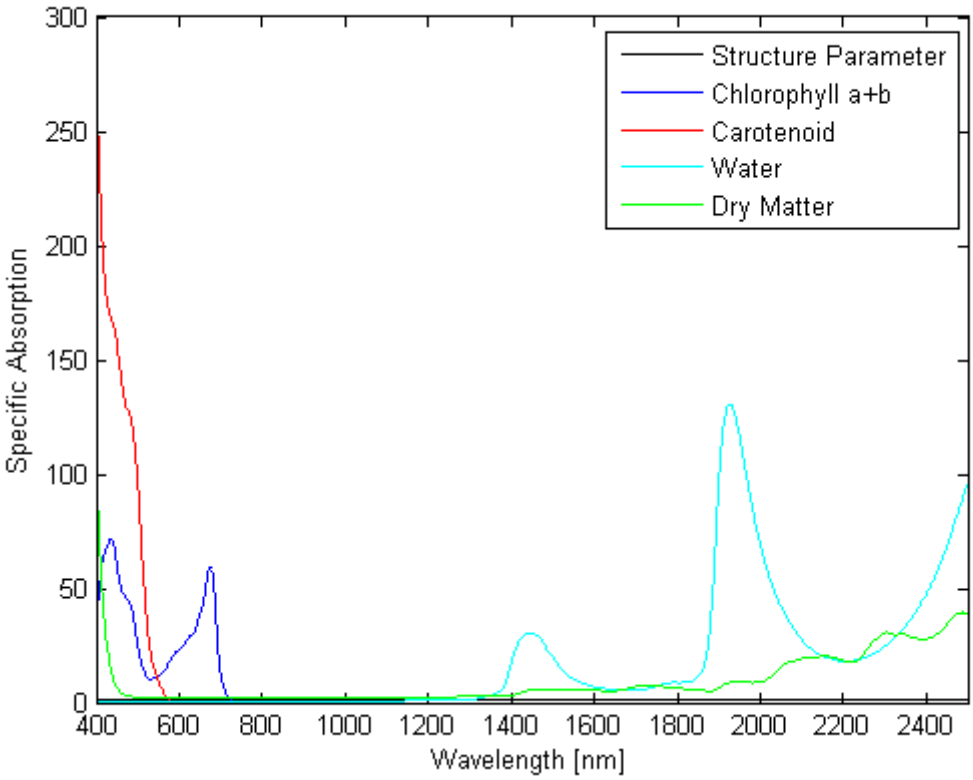
Structure Parameter
Chlorophyll a+b
Carotenoid
Water
Dry Matter
Specific Absorption
Wavelength [nm]
0
50
100
150
200
250
300
400
600
800
1000
1200
1400
1600
1800
2000
2200
2400

a

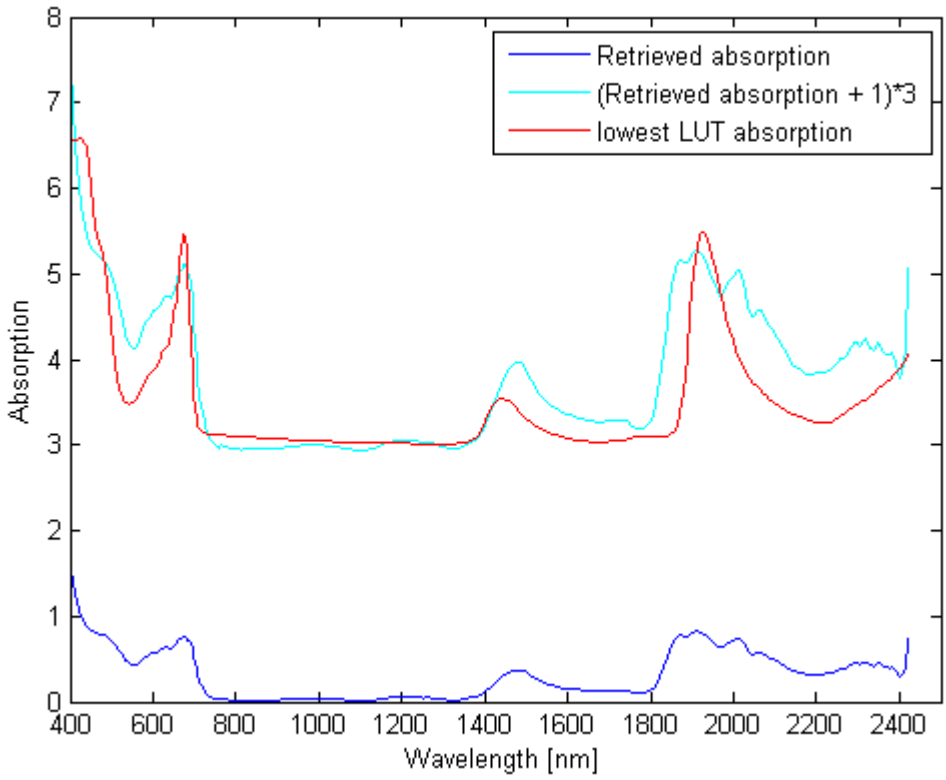
Retrieved absorption
(Retrieved absorption + 1)*3
lowest LUT absorption
Absorption
Wavelength [nm]
0
1
2
3
4
5
6
7
8
400
600
800
1000
1200
1400
1600
1800
2000
2200
2400

b

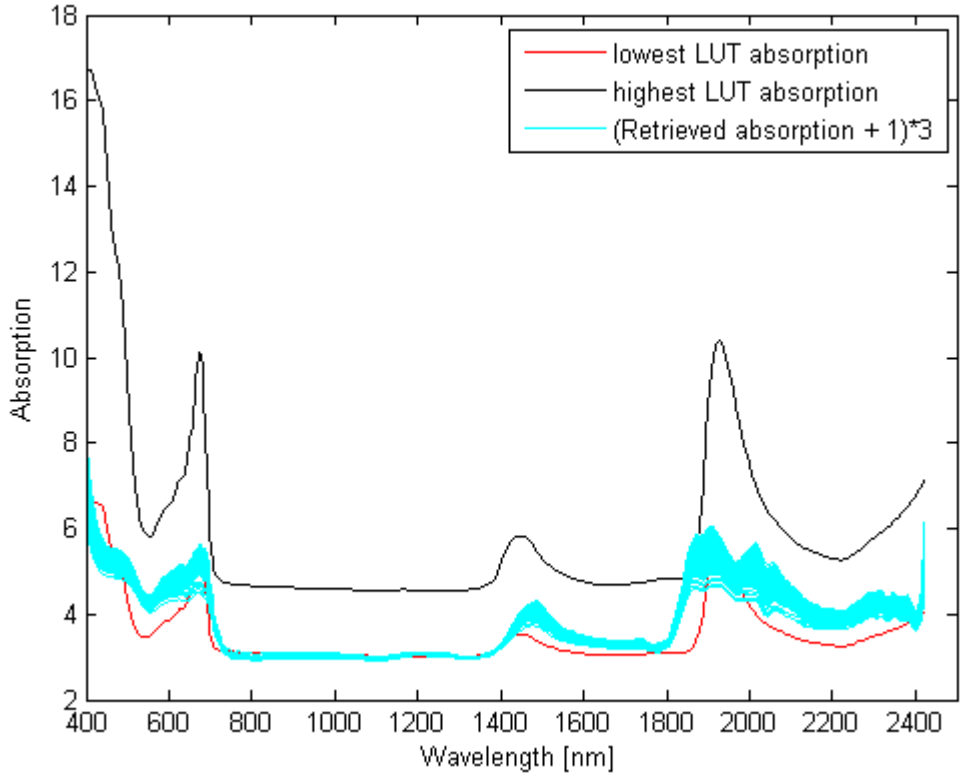

c

Figure 23. (a) Specific absorption spectra of used leaf biochemical constituents. (b) Lowest simulated LUT, retrieved and transformed retrieved absorption spectra. (c) Lowest and highest simulated LUT and all retrieved (corn field 1) absorption spectra.

The absorption spectra of all pixels of the corn field are shown by figure 23c (cyan). As expected, the absorption spectra are very similar with the only difference laying in the absorption magnitude. The similar absorption signature makes sense since all the spectra should be from the same crop type. It must be noted, however, that small shifts in x-direction (maximum 10nm) of the local maxima are found between the lower and higher absorption spectra. The lowest and highest simulated absorption spectra from the LUT are also illustrated in figure 23c. They show the superposition of the different constituent absorption as stated by the left hand side of equation (15), since both curves have the same form but with different magnitudes. Similar to figure 23b, all retrieved absorption spectra have a comparable progress to the simulated ones, once scaled by adding 1 and multiplying by 3. Again, the two peaks at 1480nm and 1910nm are slightly shifted. This effect is stronger for both peaks for the retrieved spectra with a higher absorption. Furthermore, the missing peaks in the LUT spectra are probably also due the overwhelming water absorption.

5. Discussion

5.1 Sensitivities of retrieved structural parameters

The probably most striking result of the thesis is the sensitivity of the retrieved structural parameter DASF to leaf biochemical constituents. The sensitivities of the overall recollision probability, p_1, and directional escape probability, R, are less surprising since both contain the within leaf recollision probability, p_L, which is sensitive to leaf biochemical constituents. The DASF on the contrary is a fraction for the correction of reflectance due to the loss of radiation through the canopy structure and viewing geometry and should not experience any other influences than from structural and geometrical parameters. This result, if significant and correctly interpreted, would therefore question the ability to reliably retrieve structural parameters from hyperspectral data. The reason of this bias lays in the influence of the biochemical constituents on the slope of the reflectance in the spectral range used for the retrieval (4.1.1). This spectral region is proposed by Lewis & Disney (2007), who find that each spectrum of the Boreal Ecosystem Atmosphere Study (BOREAS) (Middleton & Sullivan; 2000) and Spectral Barrax Campaign (SPARC) (Carmona et al., 2010) can be described by a reference spectrum and a set of spectral invariant parameters in this region. Since a linear relationship is also obtained for every parameter setting of the model here, this result is not questioned. However, the results from the simulated spectra illustrate clearly the inability of the tested method to retrieve structural variables reliably for varying leaf biochemical constituent concentrations. This fact challenges either the spectral region used by the retrieval or the use of the reference spectrum, both central assumptions of the retrieval. Since even one plant experiences high variations of biochemical concentrations during an annual cycle (e. g. Demarez, 1999; Ottander et al., 1995), the reliability of retrieved structural parameters is seriously doubted. Furthermore, one reason why this problematic did not arise yet is that the influence of one constituent can easily overwhelm the influence of another. Adams (2013) for example tests the influence of different leaf biochemical concentrations (chlorophyll, dry matter and equivalent water thickness) when retrieving the DASF. She finds that quiet different concentrations do have nearly no effect on the retrieval. However, she changes all three constituent concentrations at a time. Similar results to hers could be reproduced (not shown) using the PROSAIL model with her input parameters. It is also shown with the same model and algorithm, on the other hand, that changing the concentration of only one biochemical constituent at a time results in different retrieved parameter values. This further points out that the effect of one biochemical constituent concentration can be blurred through the effects of other constituent concentrations.

Despite the important bias in the retrieval, the results of the correlations between retrieved structural parameters and input structural parameters of the model are either in accord with expectations from the theory or comparable with other work. This is especially significant since not only the results between the structural variables of the model and the DASF but also the more detailed ones between structural variables of the model and p_1 and R are all in line with the theory of spectral invariants. It shows that the theory is working well nonetheless, at least for constant leaf biochemical constituent concentrations. So despite the sensitivity of the DASF to biochemical constituents of the canopy, the results indicate that the retrieval is not completely wrong. They rather show one aspect supporting the theory and the other highlighting a probable issue in the retrieval of structural variables with respect to leaf biochemical constituents.

In contrast to the simulation section, the results of the sensitivity analysis of retrieved p_1 and R from remotely sensed data of homogeneous agricultural canopy to in situ retrieved structural parameters are mostly not what is initially expected by the theory or obtained by other work. With the exception of the sky fraction, none of the sensitivities show a trend or can be brought in line with the theory. As already mentioned, the sensitivities to leaf biochemical constituents of the overall recollision and directional escape probabilities are not controlled in this analysis. The lack of relationship between spectrally and in situ retrieved structural parameters implies that the influence of the biochemical constituents must be comparable to or even larger than the influence of the structural parameters. This explains the discrepancy to the analysis with simulated spectral data and literature. The correlations between in situ retrieved structural parameters and the DASF, on the other side, show comparable but much weaker results to the ones of the simulation section. It must also be noted that the DASF values are lower compared to the mean field values of the same crop types, which is rather indicative for the influence of an unknown effect. The influence of biochemical constituents on the DASF already experienced with simulated spectra could also be present here, which would explain the much weaker relationships between DASF and in situ retrieved structural variables. It is therefore questioned if the retrieval of structural parameters from hyperspectral data of more complex canopies than perfectly homogeneous ones can be performed reliably enough with this method. On the one side, p_1 and R are affected too much by the sensitivity to leaf biochemical constituents, which drowns their sensitivity to structural variables of the canopy. On the other side, the retrieval of the DASF seems not fully coherent. Unfortunately, the analysis is not able to demonstrate whether latter originates from the sensitivity of the DASF to leaf biochemical constituents or from the augmented complexity of the canopy compared to the one of the PROSAIL model. These results nevertheless suggest that the retrieval struggles with more complex canopies containing varying leaf biochemical constituents.

Neither the sensitivity analysis between the DASF and LiDAR retrieved structural parameters nor the spectral invariant space from the forest of Lägern produce any trend or interpretable result. As for the simulated and homogeneous canopy, the sensitivity to biochemical constituents is also expected for structural parameters retrieved from heterogeneous canopy. This would explain the bad results obtained in this section. However, another issue seems to affect the results in first order. When looking at the map specifications of the data sets, the first LiDAR data set starts at the upper left corner 669660.5 / 259209.5 while the geometrically rectified APEX data starts at 664202 / 262659. This results in a shift of 0.5m since both have a spatial resolution of 2x2m. Therefore, the missing relationship between the LiDAR retrieved structural parameters of the first set and the retrieved DASF is probably due to a lacking image coregistration. The upper left corner of the second LiDAR retrieved structural parameter set is 668539 / 260380 which, again, results in a shift of 1m compared with the DASF data set. This spatial shift is probably also responsible for a lack in image coregistration and a missing relationship between the two parameters. The figures 20c and d further support this hypothesis as they show that the DASF is similarly distributed for all PAI values. This would mean that the DASF is not affected by the density of the vegetation canopy which is highly improbable. Therefore, a missing coregistration between the datasets seems very likely. Consequently, no conclusion can be drawn for the sensitivity of retrieved structural parameters to LiDAR derived structural parameters and their usability for the heterogeneous forest of the Lägern.

Other interesting findings still result from the analysis of the heterogeneous area, for example when investigating different exposed areas of the hill. As normal for the northern hemisphere, the northern side of the hill of the Lägern forest is less exposed to the sun compared to the southern side. A lot more pixels are filtered out by the shadow filter therefore, but the remaining pixels still show overall smaller DASF values than on the south side of the hill (fig. 16a and b). This result suggests a sensitivity of the retrieved structural parameters on illumination, since darker pixels result in smaller DASF values. The sensitivity would have a large impact on the application spectrum of the retrieval. Especially for hilly areas, but also forested areas in general where a lot of smaller topographical effects generate large illumination differences, the meaning of retrieved DASF would be very limited by this issue.

A similar effect is found when comparing the distributions of DASF values from the 2m resolution and the resampled 8m resolution (fig. 15). The statistic of the DASF value distribution from the 8m resolution contain more lower DASF values, which suggests resampling effects. It could be presumed that the lower resolution comprises more aggregated pixels where the theory of spectral invariants is not valid but which are mixed with good ones so that they pass through the filter. This problem is already mentioned in section 4.2.1 where mixed pixels of vegetation and bare soil are not filtered out

and show considerably lower DASF values. This hypothesis, however, is rejected by the fact that only very few pixels are filtered out by the R^2 filter in the forest at the 2m resolution. The main reason is probably the shadowing effect. The shadows in the 2m resolution scene are mostly only a few pixels large, often situated between tree crowns or on the northern side of a crown. While resampling, these shadowed areas are often mixed with more illuminated ones. The shadow mask at the resolution of 8m finds only the largest shadowed areas of the 2m resolution, while smaller ones are averaged out during the resampling. Therefore, more shadowed areas of the 2m resolution are not filtered in the 8m resolution which causes a larger number of slightly darker pixels. Darker pixels lead to a shift towards lower DASF values as discussed by the last paragraph. This further demonstrates how resampling can affect the retrieval of structural parameters.

5.2 Impact of high spatial resolution

Another issue regarding the retrieval of structural parameters is concerning the goodness (R^2) of the linear relationship between HCRF/ω and HCRF. The R^2 should be an indication for the validity of the applicability of the theory of spectral invariants on a pixel. In the analysis of the homogeneous canopy, however, an ideal threshold value for the filtering of pixels with too low R^2 could not be found. If the threshold is set to a value where all bare soil pixels are removed, a lot of vegetation pixels are removed as well. Especially the grass types are vulnerable to higher threshold values. On the other side, a lower threshold value includes too many bare soil pixels which exhibit very low DASF values as shown by figure 8. There is probably still enough vegetation signature in the reflectance of these pixels so that the linear fit of the DASF retrieval is valid. However, the theory of spectral invariants should not be valid for the mentioned pixels since they are brown in the true colour scene and therefore certainly not a saturated vegetation pixel. This illustrates another challenge of the retrieval where the spectral range between 710nm and 790nm is apparently not enough to clearly separate dense vegetation from sparse one. It is suspected that the cause for the difficulties mentioned above are the small spatial resolution and eventual effects at this scale not considered by the theory or retrieval.

As presented in section 4.2.4, the results of the spectral invariant space are very different depending on the number of aggregated pixels. When taking mean values of retrieved parameters from a field, the resulting spectral invariant space can be reasonably interpreted and seems therefore to make sense. Corn is namely separable from the other crop types on the micro scale, while a similar range

of macro scale values is taken up by all crop types. This result is comparable to the one of Carmona et al. (2010), where corn is the only crop type distinguishable from the others. However, when taking the same data on plot level (6x6m), a different distribution of values is obtained in the spectral invariant space. The result also makes less sense and shows a weak trend for corn. Other studies (e. g. Knyazikhin et al., 2009; Schull et al., 2011; Wang et al., 2011), however, applying the theory of spectral invariants on reflectance data do not encounter this problem. The studied canopies are, however, forested areas which better meet the requirement of a dense canopy bounded from below by a non-reflecting background. In addition, most of these studies work with data on a spatial resolution between 15.7m (Schull et al., 2011) and 500m (Wang et al., 2010). However, one study (Knyazikhin et al., 2009) successfully discriminates tree species from forest reflectance data using retrieved structural parameters on a comparable resolution (3.3m) than used here. It is thus not clear whether the issues experienced in this thesis are the result of using reflectance data of an agricultural canopy, which eventually does not fully meet the requirements of dense vegetation, or the small spatial resolution where the sensitivity of retrieved structural parameters is too strong. It is assumed that the issues are linked to the sensitivities of retrieved overall recollision and directional escape probabilities to biochemical constituents as already argued in 5.1. This is particularly apparent on high resolution as for example the plot level data as explained in the following and leads to incoherent results for the spectral invariant space. The results are much better when taking the mean values of retrieved structural parameters from a whole field. It is hypothesised that the reason for the improvement when using lower resolution data is probably the aggregation of the variation of biochemical constituent concentrations within a pixel. Biochemical constituents do still influence the values of p_1 and R, though. However, the distribution of constituent concentrations can probably be assumed constant between the fields of one crop type considering the large numbers of averaged pixels in every field. This reduces the effect of biochemical constituents on p_1 and R for each of the crop types, which in turn leads to relatively coherent results. The analysis of crop discrimination using the spectral invariant space conducted here on plot level comprises only 20 measurements in total, while Knyazikhin et al. (2009) use much more pixels in their analysis. The number of measurements used by this thesis is by far insufficient to be able to neglect outliers. Therefore, the bad result from the plot level analysis should be taken into account with care. The analysis on field level consists not of too many measurements neither, but the measurements themselves are mean values from a large number of pixels. The spatial resolution could hence have a central impact on the application of the spectral invariants theory on reflectance data as suggested by these results. Further, the impact of the sensitivity of applications of the spectral invariants theory to leaf biochemical constituents needs absolutely more investigation. Especially the transition area of the

resolution where biochemical sensitivities could be neglected due to statistical considerations would be of large interest and eventually a resort to the challenges illustrated here.

5.3 Leaf biochemical constituent retrieval

The analysis of the chlorophyll retrieval using a leaf level model presents the evidence highlighted by many papers about the need of a correction for canopy structural effects of reflectance data. The retrieval of Gitelson et al. (2006) works perfectly on leaf level reflectance, but fails by far to predict chlorophyll concentration when a canopy structure is added. However, a linear correction of the retrieved chlorophyll concentrations with the DASF seems not possible. The reason is the different forms of the progressions of retrieved chlorophyll concentration values and DASF values for varying LAI. No other model has been tested; however, a correction of retrieved chlorophyll concentrations with the DASF is, at least from a conceptual point of view, senseless since the DASF represents a correction factor for reflectance data and not for a product of latter. Another idea would therefore be to apply the DASF linearly on the reflectance data as intended and use Gitelson et al.'s three band model with the corrected reflectance. However, the formula can be rearranged (formula (4) of Gitelson et al., 2006). Through the resulting band ratio and the suggested bands for the retrieval of the chlorophyll pigments, the DASF is multiplied in the numerator and the denominator and consequently cancel itself down in the fraction. Therefore, no correction is obtained and the model is still biased for canopy level reflectance data.

The attempt to retrieve leaf biochemical constituent concentrations using derivations from the spectral invariants theory leads to promising first results, but needs further effort to obtain a satisfying and applicable method. The curves of retrieved and simulated absorption spectra illustrate a similar progress throughout the absorption spectra. The absorption features of the different constituents used in the simulations are relatively well visible in the retrieved spectra and no additional absorption feature is strikingly apparent. This indicates that the used constituents seem to compose the most important absorption elements and that retrieved absorption spectra can probably be reconstructed as the superposition of the product of specific absorption coefficient and respective constituent concentration as stated by equation (15). Nevertheless, important challenges are encountered, which prevent reliable retrievals of leaf biochemical constituents so far. One is the difference of the absorption intensities between simulated and retrieved absorption. It seems as if there is first a shift of the whole retrieved spectrum in y-direction and then also a stretch of the

peaks. By applying a linear transformation to the retrieved spectra, they get comparable to the simulated spectra. However, it is not clear why such large differences between simulated and retrieved spectra occur. It is also unsolved where the exact origin of this transformation is situated and therefore what the exact transformation of each spectrum is. The first shift is probably due to the structure parameter. Its absorption is relatively constant over the whole spectrum. A wrong parametrisation of the structure parameter therefore leads to a shift of the whole spectrum in positive y-direction because of the principle of superposition. The difference in the absorption intensities of the peaks is then presumably an issue of the concentrations of the remaining biochemical constituents. Although the probable reason of the difference between retrieved and simulated absorption spectra seems obvious, the cause is still vague. It is unclear whether the retrieved or simulated spectrum is the correct one and why the wrong one is scaled compared to the correct one. A further remaining challenge is the shift in x-direction of certain peaks. Assuming a solution for the first challenge, even if the two absorption spectra laid on a comparable position in y-direction, the shifts of the local maxima would impede an exact comparison between retrieved and simulated spectrum wavelength wise. Therefore, the retrieval of leaf biochemical constituents would still experience challenges. Again, the reason for the shift of certain peaks remains unclear. The simulated spectra have been convoluted to match the wavelengths of the APEX sensor. Since the spectra are absorption and not reflection, it is thus questioned if the convolution also works reliably for absorption spectra.

With regard to the first part of the thesis, further points have to be considered regarding the retrieved structural parameters used in the retrieval of biochemical constituents. For this analysis the mean values of retrieved structural parameters from one field are used. As discussed in 5.2, the sensitivity of retrieved parameters to leaf biochemical constituents is probably reduced for a large number of aggregated pixels. However, this has two further implications for the retrieval of leaf biochemical constituents. First, the general applicability of such a retrieval for remote sensing data is reduced since another piece of information is needed. This information, the classification of a pixel to a crop or tree species, is needed for the aggregation of the pixels. The results of this study suggest that without this process, the influence of the sensitivity of retrieved parameters to biochemical constituents is too important. However, even if this sensitivity is reduced through the aggregation, the retrieved structural parameters are still dependent to biochemical constituents. Since the structural parameters are used in the retrieval of biochemical constituents, latter are themselves dependent on present biochemical constituents of the canopy, which is of course problematic.

In addition to the implications of the sensitivity of retrieved structural parameters, another fundamental problematic needs attention. Even if the sensitivities could be fully eliminated through a

revised retrieval, both retrievals would be performed on the same underlying data. This would still represent an obstacle for the reliability of retrieved biochemical constituents because of the dependence of the two retrievals. Therefore, the postulate of Lewis & Disney (2007) is probably true and the exact retrieval of both, structural parameters and leaf biochemical constituents is fundamentally not possible for spectral data without additional information. This postulate, which is further supported by this thesis, suggests that for the retrieval of leaf biochemical constituents from remotely sensed spectral data at least one additional independent measurement of the same vegetation canopy is indispensable. Possibilities could consist of multiangle spectral measurements or a simulation approach using LiDAR measurements for the canopy structure model combined with spectroscopic measurements for the spectral response of the canopy.

6. Conclusion

This thesis presents multiple investigations of the sensitivity of spectral invariants theory applications to leaf biochemical and canopy structural parameters to assign the possibility of estimating leaf biochemical constituent contents from hyperspectral remote sensing data that are corrected for canopy structural effects. The application of the theory of spectral invariants comprises the retrieval of structural parameters from high resolution hyperspectral data, namely the DASF, the overall recollision probability, p_1, and the directional escape probability, R, as well as crop/canopy type discrimination using the spectral invariant space.

Beneath sensitivities of the DASF to illumination and resampling, the most striking findings are the rather large sensitivities of retrieved structural parameters on leaf biochemical constituents. These results challenge severely the assumptions of the retrieval and have huge impacts on usability and significance of spectral invariants applications. The sensitivity is less surprising for p_1 and R, but the magnitude of the sensitivity to leaf biochemical constituents is at least as important as the sensitivity of the two parameters to canopy structural parameters. However, the sensitivity of the DASF to leaf biochemical constituents found in this thesis is probably a worst case result for the application of the theory of spectral invariants. The applications of the theory seem nevertheless to work for idealised canopies and spectral data, however, the results of this thesis suggest only under two conditions:

1. The content of leaf biochemical constituents can be controlled.
2. The spatial resolution is large enough to aggregate enough variation of leaf biochemical constituent concentrations, which reduces the sensitivity.

Despite the critiques on the application, the correctness of the theory of spectral invariants is neither challenged nor doubted.

The attempt to retrieve leaf biochemical constituents from hyperspectral remote sensing data using retrieved structural parameters seems promising at first sight since simulated and retrieved absorption spectra come relatively close. However, besides challenges still experienced during the retrieval, the implications of the sensitivities of structural parameters make a reliable retrieval for leaf biochemical constituents impossible without additional information. At least two independent measurements are therefore suggested for the simultaneous retrieval of canopy structural and leaf biochemical constituents.

7. References

Adams, J. (2013). Empirically testing the use of Directional Area Scattering Factor (DASF) to correct hyperspectral remote sensing data for canopy structural effects. University College London.

Andrew, M. E., Wulder, M. A., & Nelson, T. A. (2014). Potential contributions of remote sensing to ecosystem service assessments. *Progress in Physical Geography*, *38*(3), 328–353.

Baret, F., Jacquemoud, S., Guyot, G., & Leprieur, C. (1992). Modeled analysis of the biophysical nature of spectral shifts and comparison with information content of broad bands. *Remote Sensing of Environment*, *41*(2), 133-142.

Blackburn, G. A. (2007). Hyperspectral remote sensing of plant pigments. *Journal of Experimental Botany*, *58*(4), 855–867.

Carmona, P. L., Schull, M., Knyazikhin, Y., & Pla, F. (2010). The application of spectral invariants for discrimination of crops using CHRIS-PROBA data. *Hyperspectral Image and Signal Processing: Evolution in Remote Sensing (WHISPERS)*, 2010 2nd Workshop on, 1–4, IEEE.

Costanza, R., d'Arge, R., de Groot, R., Farber, S., Grasso, M., Hannon, B., … van den Belt, M. (1997). The value of the world's ecosystem services and natural capital. *Nature*, *387*(6630), 253–260.

Curran, P. J. (1989). Remote sensing of foliar chemistry. *Remote Sensing of Environment*, *30*(3), 271–278.

Demarez, V. (1999). Seasonal variation of leaf chlorophyll content of a temperate forest. Inversion of the PROSPECT model. *International Journal of Remote Sensing*, *20*(5), 879–894.

Gitelson, A. A., Gritz, Y., & Merzlyak, M. N. (2003). Relationships between leaf chlorophyll content and spectral reflectance and algorithms for non-destructive chlorophyll assessment in higher plant leaves. *Journal of Plant Physiology*, *160*(3), 271–82.

Gitelson, A. A., Keydan, G. P., & Merzlyak, M. N. (2006). Three-band model for noninvasive estimation of chlorophyll, carotenoids, and anthocyanin contents in higher plant leaves. *Geophysical Research Letters*, *33*(11).

Heiskanen, J. (2006). Tree cover and height estimation in the Fennoscandian tundra–taiga transition zone using multiangular MISR data. *Remote Sensing of Environment*, *103*(1), 97–114.

Holst, T., Hauser, S., Kirchgäßner, A., Matzarakis, A., Mayer, H., & Schindler, D. (2004). Measuring and modelling plant area index in beech stands. *International Journal of Biometeorology*, *48*(4), 192–201.

Homolová, L., Malenovský, Z., Clevers, J. G. P. W., García-Santos, G., & Schaepman, M. E. (2013). Review of optical-based remote sensing for plant trait mapping. *Ecological Complexity*, *15*, 1–16.

Houborg, R., Fisher, J. B., & Skidmore, A. K. (2015). Advances in remote sensing of vegetation function and traits. *International Journal of Applied Earth Observation and Geoinformation, 43*, 1-6.

Huang, D., Knyazikhin, Y., Dickinson, R. E., Rautiainen, M., Stenberg, P., Disney, M., … Myneni, R. B. (2007). Canopy spectral invariants for remote sensing and model applications. *Remote Sensing of Environment*, *106*(1).

Hueni, A., Lenhard, K., Baumgartner, A., & Schaepman, M. E. (2013). Airborne Prism Experiment Calibration Information System. *Geoscience and Remote Sensing, IEEE Transactions on*.

Itten, K. I., Dell'Endice, F., Hueni, A., Kneubühler, M., Schläpfer, D., Odermatt, D., … Meuleman, K. (2008). APEX - the Hyperspectral ESA Airborne Prism Experiment. *Sensors*, *8*(10), 6235–6259.

Jacquemoud, S., & Baret, F. (1990). PROSPECT: A model of leaf optical properties spectra. *Remote Sensing of Environment*, *34*(2), 75–91.

Kimes, D. S., Ranson, K. J., Sun, G., & Blair, J. B. (2006). Predicting lidar measured forest vertical structure from multi-angle spectral data. *Remote Sensing of Environment*, *100*(4), 503–511.

Knyazikhin, Y. (2013). On the Radiative Transfer Based Remote Sensing of Forest Structure and Leaf Biochemistry. *AGU Fall Meeting Abstracts*, C5.

Knyazikhin, Y., Marshak, A., & Myneni, R. B. (2005). 3D Radiative Transfer in Vegetation Canopies and Cloud-Vegetation Interaction. In A. Marshak & A. Davis (Eds.), *3D Radiative Transfer in Cloudy Atmospheres, 14*(pp. 617–651). Springer Berlin Heidelberg.

Knyazikhin, Y., Martonchik, J. V, Myneni, R. B., Diner, D. J., & Running, S. W. (1998). Synergistic algorithm for estimating vegetation canopy leaf area index and fraction of absorbed photosynthetically active radiation from MODIS and MISR data. *Journal of Geophysical Research: Atmospheres (1984–2012), 103*(D24), 32257-32275.

Knyazikhin, Y., Schull, M. A., Stenberg, P., Mõttus, M., Rautiainen, M., Yang, Y., … Myneni, R. B. (2013). Hyperspectral remote sensing of foliar nitrogen content. *Proceedings of the National Academy of Sciences* , *110* (3).

Knyazikhin, Y., Schull, M. A., Xu, L., Myneni, R. B., & Samanta, A. (2011). Canopy spectral invariants. Part 1: A new concept in remote sensing of vegetation. *Journal of Quantitative Spectroscopy and Radiative Transfer*, *112*(4), 727–735.

Knyazikhin, Y., Schull, M., Hu, L., Myneni, R., & Carmona, P. L. (2009). Canopy spectral invariants for remote sensing of canopy structure. *Hyperspectral Image and Signal Processing: Evolution in Remote Sensing, 2009. WHISPERS'09. First Workshop on* (pp. 1-4). IEEE.

Latorre-Carmona, P., Knyazikhin, Y., Alonso, L., Moreno, J. F., Pla, F., & Yan, Y. (2014). On Hyperspectral Remote Sensing of Leaf Biophysical Constituents: Decoupling Vegetation Structure and Leaf Optics Using CHRIS–PROBA Data Over Crops in Barrax. *Geoscience and Remote Sensing Letters, IEEE*, *11*(9), 1579-1583.

Leiterer, R., Furrer, R., Schaepman, M. E., & Morsdorf, F. (2015). Forest canopy-structure characterization: A data-driven approach. *Forest Ecology and Management*, *358*, 48–61.

Lewis, P., & Disney, M. (2007). Spectral invariants and scattering across multiple scales from within-leaf to canopy. *Remote Sensing of Environment*, *109*(2), 196–206.

Liebisch, F., Küng, G., Damm, A., & Walter, A. (2014). Characterization of crop vitality and resource use efficiency by means of combining imaging spectroscopy based plant traits. *Workshop on Hyperspectral Image and Signal Processing, Evolution in Remote Sensing (Vol. 6)*.

Middleton, E., & Sullivan, J. (2000). BOREAS TE-10 leaf optical properties for SSA species. Data set. Available on-line [http://www. daac. ornl. gov] from Oak Ridge National Laboratory Distributed Active Archive Center, Oak Ridge, Tennessee, USA.

Mõttus, M. (2007). Photon recollision probability in discrete crown canopies. *Remote Sensing of Environment*, *110*(2), 176–185.

Myneni, R. B., Maggion, S., Iaquinta, J., Privette, J. L., Gobron, N., Pinty, B., … Williams, D. L. (1995). Optical remote sensing of vegetation: Modeling, caveats, and algorithms. *Remote Sensing of Environment*, *51*(1), 169–188.

Ottander, C., Campbell, D., & Öquist, G. (1995). Seasonal changes in photosystem II organisation and pigment composition in Pinus sylvestris. *Planta*, *197*(1), 176–183.

Panferov, O., Knyazikhin, Y., Myneni, R. B., Szarzynski, J., Engwald, S., Schnitzler, K. G., & Gravenhorst, G. (2001). The role of canopy structure in the spectral variation of transmission and absorption of solar radiation in vegetation canopies. *Geoscience and Remote Sensing, IEEE Transactions on*, *39*(2), 241-253.

Rautiainen, M., Mõttus, M., & Stenberg, P. (2009). On the relationship of canopy LAI and photon recollision probability in boreal forests. *Remote Sensing of Environment*, *113*(2), 458–461.

Rautiainen, M., Stenberg, P., Nilson, T., & Kuusk, A. (2004). The effect of crown shape on the reflectance of coniferous stands. *Remote Sensing of Environment*, *89*(1), 41–52.

Richter, R., & Schläpfer, D. (2004). *Atmospheric / Topographic Correction for Airborne Imagery. ATCOR-4 User Guide Version.* Wessling, Germany: DLR - German Aerospace Center.

Schläpfer, D., Schaepman, M. E., & Itten, K. I. (1998). PARGE: parametric geocoding based on GCP-calibrated auxiliary data. In *SPIE's International Symposium on Optical Science, Engineering, and Instrumentation* (pp. 334-344). International Society for Optics and Photonics.

Schneider, F. D., Leiterer, R., Morsdorf, F., Gastellu-Etchegorry, J.-P., Lauret, N., Pfeifer, N., & Schaepman, M. E. (2014). Simulating imaging spectrometer data: 3D forest modeling based on LiDAR and in situ data. *Remote Sensing of Environment*, *152*, 235–250.

Schull, M. A., Ganguly, S., Samanta, A., Huang, D., Shabanov, N. V, Jenkins, J. P., … Knyazikhin, Y. (2007). Physical interpretation of the correlation between multi-angle spectral data and canopy height. *Geophysical Research Letters*, *34*(18).

Schull, M. A., Knyazikhin, Y., Xu, L., Samanta, A., Carmona, P. L., Lepine, L., … Myneni, R. B. (2011). Canopy spectral invariants, Part 2: Application to classification of forest types from hyperspectral data. *Journal of Quantitative Spectroscopy and Radiative Transfer*, *112*(4), 736–750.

Schull, M., Ganguly, S., Samanta, A., Jenkins, J., Knyazikhin, Y., Myneni, R. B., & Huang, D. (2007). Retrieving 3D canopy structure from synergistic analysis of multi-angle and lidar data. *Geoscience and Remote Sensing Symposium, 2007. IGARSS 2007. IEEE International*.

Sims, D. A., & Gamon, J. A. (2002). Relationships between leaf pigment content and spectral reflectance across a wide range of species, leaf structures and developmental stages. *Remote Sensing of Environment*, *81*(2-3), 337–354.

Smolander, S., & Stenberg, P. (2005). Simple parameterizations of the radiation budget of uniform broadleaved and coniferous canopies. *Remote Sensing of Environment*, *94*(3), 355–363.

Stenberg, P. (2007). Simple analytical formula for calculating average photon recollision probability in vegetation canopies. *Remote Sensing of Environment*, *109*(2), 221–224.

Verhoef, W. (1984). Light scattering by leaf layers with application to canopy reflectance modeling: The SAIL model. *Remote Sensing of Environment*, *16*(2), 125–141.

Wang, Z., Schaaf, C. B., Lewis, P., Knyazikhin, Y., Schull, M. A., Strahler, A. H., … Blair, B. J. (2011). Retrieval of canopy height using moderate-resolution imaging spectroradiometer (MODIS) data. *Remote Sensing of Environment*, *115*(6), 1595–1601.

Wang, Z., Schaaf, C. B., Philip, L., Knyazikhin, Y., Schull, M. A., Strahler, A. H., … Chopping, M. (2010). Canopy vertical structure using MODIS Bidirectional Reflectance data. In *Hyperspectral Image and Signal Processing: Evolution in Remote Sensing (WHISPERS), 2010 2nd Workshop on* (pp. 1-4). IEEE.

Zhang, Y., Chen, J. M., Miller, J. R., & Noland, T. L. (2008). Leaf chlorophyll content retrieval from airborne hyperspectral remote sensing imagery. *Remote Sensing of Environment*, *112*(7), 3234–3247.

8. Personal declaration

I hereby declare that the submitted thesis is the result of my own, independent work. All external sources are explicitly acknowledged in the thesis.